2001

Characterization of the human rod photoreceptor cyclic GMP phosphodiesterase alpha subunit gene promoter.

Kathryn Hanson Shows
University of Alabama at Birmingham

INFORMATION TO USERS

This manuscript has been reproduced from the microfilm master. UMI films the text directly from the original or copy submitted. Thus, some thesis and dissertation copies are in typewriter face, while others may be from any type of computer printer.

The quality of this reproduction is dependent upon the quality of the copy submitted. Broken or indistinct print, colored or poor quality illustrations and photographs, print bleedthrough, substandard margins, and improper alignment can adversely affect reproduction.

In the unlikely event that the author did not send UMI a complete manuscript and there are missing pages, these will be noted. Also, if unauthorized copyright material had to be removed, a note will indicate the deletion.

Oversize materials (e.g., maps, drawings, charts) are reproduced by sectioning the original, beginning at the upper left-hand corner and continuing from left to right in equal sections with small overlaps.

Photographs included in the original manuscript have been reproduced xerographically in this copy. Higher quality 6" x 9" black and white photographic prints are available for any photographs or illustrations appearing in this copy for an additional charge. Contact UMI directly to order.

ProQuest Information and Learning
300 North Zeeb Road, Ann Arbor, MI 48106-1346 USA
800-521-0600

UMI®

CHARACTERIZATION OF THE HUMAN ROD PHOTORECEPTOR CYCLIC GMP PHOSPHODIESTERASE ALPHA SUBUNIT GENE PROMOTER

by

KATHRYN HANSON SHOWS

A DISSERTATION

Submitted to the graduate faculty of The University of Alabama at Birmingham,
in partial fulfillment of the requirements for the degree of
Doctor of Philosophy

BIRMINGHAM, ALABAMA

2001

ProQuest Information and Learning Company
300 North Zeeb Road
P.O. Box 1346
Ann Arbor, MI 48106-1346

ABSTRACT OF DISSERTATION
GRADUATE SCHOOL, UNIVERSITY OF ALABAMA AT BIRMINGHAM

Degree Ph.D. Program Vision Science

Name of Candidate Kathryn Hanson Shows

Committee Chair Thomas Norton

Title Characterization of the Human Rod Photoreceptor Cyclic GMP Phosphodiesterase Alpha Subunit Gene Promoter

Rod photoreceptor cyclic guanosine monophosphate (cGMP) phosphodiesterase (PDE6) is an enzyme consisting of alpha, beta, and two gamma subunits involved in mammalian phototransduction. PDE6 controls the turnover rate of cGMP to GMP within rod outer segments. The second messenger cGMP binds and opens gated ion channels in the rod cell membrane. When light activates phototransduction, PDE6 cleaves cGMP, closing the channels and hyperpolarizing the membrane.

Deficiencies of PDE6 lead to retinal disorders such as retinitis pigmentosa (RP) and congenital stationary night blindness (CSNB). Disease-causing mutations lie within the coding regions of alpha and beta subunit genes. Identification of regulatory regions of these subunits may contribute to *in vivo* replacement using gene therapy.

Rhodopsin, arrestin, transducin, and PDE6 beta subunit demonstrate photoreceptor-specific transcription. A binding site for the transcription factor cone-rod homeobox (CRX) is essential for rod-specific transcription. The transcription factor neural retina leucine (NRL) zipper is necessary for upregulating rhodopsin transcription. Sequencing of the PDE6 alpha (PDE6A) subunit proximal promoter revealed a CRX-binding element (CBE), a TATA-like binding site, and a NRL binding element (NRE)-like site. CBE,

TATA-like, and NRE-like sites are within a CRX-footprinted region. Thus, it was hypothesized that both CRX and NRL are necessary for transcription of PDE6A.

Transgenic mouse studies showed transcription of a 300-bp region surrounding the transcription start point in inner segments of photoreceptors. Transient transfections demonstrated transactivation by CRX and NRL on PDE6A promoter expression plasmids. CRX and NRL together exhibit a synergistic effect on PDE6A transactivation. Electrophoretic mobility shift assay demonstrated CRX binding to CBE, TATA-like, or NRE-like oligonucleotides that contain the CRX core sequence TAAT. CRX binds more strongly to the CBE site than to either the TATA-like or NRE-like sites. Mutagenesis of the CBE rather than the TATA had a greater effect on CRX binding. Semi-quantitative reverse transcription PCR demonstrated PDE6A expression at 60% of normal levels in mice without CRX expression.

This study demonstrates that a 300-bp promoter of the PDE6A gene contains binding sites sufficient to drive transcription in photoreceptors *in vivo* through the interaction of CRX, NRL, and related factors.

ACKNOWLEDGEMENTS

This project could not have been accomplished without the work of several people. I wish to thank Russell Taylor for his work on plasmid design for both transfections and transgenic mice: Russ laid the groundwork for the entire project. Kathy Bonness generated the mutant plasmids for the transfection studies. Brandon White also designed many of the plasmids used, as well as taught me everything I needed to know about cell culture and transfection experimental design. Mark Casillas in Dr. Trygve Tollefsbol's lab gave me tips on EMSA experimental design. Chris Anderson taught me about protein purification and running the perfect protein gel. Xuemei Zhu in Dr. Cheryl Craft's lab also gave me important guidance in purification of CRX protein from bacterial cells. Patricia Coan assisted with mouse care and dissection.

Collaborators on this project supplied invaluable materials and data. Dr. Shiming Chen and Dr. Don Zack performed the CRX footprinting studies on the PDE6A promoter. Dr. Chen also supplied purified CRX homeodomain protein and antibody for the EMSA experiments as well as important advice on transfection experimental design. Dr. Connie Cepko supplied the *Crx-/-* mice. Dr. Anand Swaroop supplied NRL expression plasmids as well as purified NRL protein and antibody for EMSA experiments. Dr. Cheryl Craft supplied bacterial stock containing the entire CRX protein in an expression plasmid for the purpose of purification.

My instructors, past and present, also contributed greatly to the success of this project. I would like to thank the Department of Medical Genetics, especially Drs. Jerry

Thompson, Rodney Go, and Rodney Perry, for their instruction and guidance early in my career. Many thanks also to the Department of Physiological Optics, especially Dr. Kent Keyser for his guidance later. I would also like to thank my committee for their diligence and hurried guidance: I appreciate the extreme effort they have made to satisfy my need for a compressed timeline of study. Dr. Trygve Tollefsbol gave invaluable advice in all areas of the project. Dr. Shu-Zhen Wang helped to troubleshoot RNA quantitation experiments. Dr. Om Srivastava advised me in protein purification as well as RNA quantitation. Dr. Thomas Norton served well as committee chairman and organizer of ideas. Dr. Steven Pittler guided the entire project as a part of his own research goals.

Lastly, I would like to thank my family and friends for their support throughout this endeavor. Without their support and encouragement I would not have come this far. And, finally, I would like to thank my husband, Josh, for his compassion, understanding, and endless telephone calls from Virginia.

TABLE OF CONTENTS

Page

ABSTRACT ii

ACKNOWLEDGEMENTS iv

LIST OF TABLES viii

LIST OF FIGURES ix

LIST OF ABBREVIATIONS xi

INTRODUCTION 1

The Phototransduction Cascade 3
Rhodopsin 5
Transducin 5
PDE6 6
Cyclic GMP as second messenger 7
Recovery after phototransduction 9
Transcription 9
Retina-Specific Transcription 10
Retinal Transcription Factors 12
Rod Photoreceptor-Specific Promoter Studies 17

RATIONALE 21

Specific Aim 1 21
Specific Aim 2 23
Specific Aim 3 31

MATERIALS AND METHODS 36

Specific Aim 1 36
Extraction of RNA from mouse retinas 36
Reverse transcription of total RNA 36
Amplification of cDNA 39
Semi-quantitative RT-PCR 39

TABLE OF CONTENTS (Continued)

Page

Specific Aim 2 41
Generation of promoter plasmid constructs 41
Tissue culture of HEK 293 cells 42
Transfections in HEK 293 cells 43
Luciferase assay of cell extracts 43
Renilla luciferase assay 44
Analysis of transfection assay results 45
Oligonucleotide preparation for EMSA 45
Protein preparation for EMSA 45
EMSA 47
Specific Aim 3 48
Transgene construct 48
Transgenic mice 49
Extraction of genomic DNA from tail samples 51
Genotyping of transgene 52
Genotyping of *rd* allele 52
Determination of the integrity of the transgene 53
β-galactosidase detection assay 56
Reverse transcriptase-PCR 56

RESULTS 58

Specific Aim 1 58
Specific Aim 2 60
Specific Aim 3 76

DISCUSSION 80

Specific Aim 1 80
Specific Aim 2 82
Specific Aim 3 87

CONCLUSIONS 90

REFERENCES 92

APPENDIX: IACUC APPROVAL 97

LIST OF TABLES

Table		Page
1	Transcription factor binding sites and consensus sequences	14
2	Primer sequences used in PCR experiments	37
3	Primer sequences used in RT-PCR experiments	40
4	Representative scheme for transfection in HEK 293 cells	44
5	Sequences of oligonucleotides used in EMSA	46
6	Representative scheme for EMSA	48
7	Relative transcript levels in 10-day-old *Crx-/-* mouse retina as compared to 10-day-old control *rd/+* mouse retina	60

LIST OF FIGURES

Figure		Page
1	Structure of cone and rod photoreceptors	2
2	The phototransduction cascade	4
3	Comparison of proximal promoter regions in known retina-specific genes	13
4	Sequence of the PDE6A proximal promoter region	19
5	Comparison of PDE6A promoter constructs used in transfection studies	26
6	CRX footprinting of the PDE6A promoter	28
7	Mutations generated in the pGL3-300 plasmid	29
8	Location of EMSA oligonucleotides	32
9	Construct of fragment used to generate transgenic mice	35
10	*Crx-/-* 10- to 11-day-old mouse retina RNA samples used in RT-PCR	38
11	Transgenic construct showing primer locations	50
12	Representative genotyping of transgenic mice with primer pair USalF/M13R	54
13	Representative genotyping of *rd/rd* mice	55
14	Presence of specific transcripts in *Crx-/-* mice	59
15	Effects of transcription factors CRX and NRL on PDE6A promoter fragments of 260-, 300-, and 1060-bp length in transient transfection experiments	62
16	Effects of both transcription factors CRX and NRL together on PDE6A promoter fragments of 260-, 300-, and 1060-bp length in transient transfection experiments	63

LIST OF FIGURES (Continued)

Figure		Page
17	Effects of transcription factors CRX and NRL on PDE6A mutant promoter fragments M13 and M16 in transient transfection experiments as compared with the 300-bp PDE6A promoter fragment	65
18	Effects of both transcription factors CRX and NRL together on PDE6A mutant promoter fragments M13 and M16 in transient transfection experiments as compared with the 300-bp PDE6A promoter fragment	66
19	Effect of mathematical correction on experimental fold stimulation values for CRX and NRL	68
20	Effect of mathematical correction on experimental fold stimulation values for CRX and NRL combined	69
21	EMSA of the truncated CRX homeodomain protein with labeled oligonucleotides	70
22	Competition with unlabeled oligonucleotides against short, labeled oligonucleotides	71
23	Competition with unlabeled oligonucleotides against medium-sized, labeled oligonucleotides	72
24	NRL binding to and competition with unlabeled oligonucleotides against long, labeled oligonucleotides	73
25	Presence of transcript in transgene-positive mouse retina	77
26	*In situ* hybridization analysis of transgene-specific transcript in transgene-positive mouse retina	79

LIST OF ABBREVIATIONS

cGMP	3', 5' cyclic guanosine monophosphate
PDE6	cGMP phosphodiesterase type VI
PDE6A	cGMP phosphodiesterase type VI alpha subunit
PDE6B	cGMP phosphodiesterase type VI beta subunit
hnRNA	heteronuclear RNA
tsp	transcription start point
CRX	cone-rod homeobox factor
CBE	CRX binding element
NRL	neural retina leucine
NRE	NRL response element
IRBP	interphotoreceptor retinoid binding protein
RPRR	rhodopsin proximal promoter region
RER	rhodopsin enhancer region
CRE	cAMP response element
RT-PCR	reverse transcriptase polymerase chain reaction
GAPDH	glyceraldehyde-3-phosphate dehydrogenase
CMV	cytomegalovirus
EMSA	electrophoretic mobility shift assay
DMEM	Dulbecco's modified eagle's medium

INTRODUCTION

Human vision, like all mammalian vision, depends on an intracellular signaling cascade within the retina, which converts light into neural signals that travel via the optic nerve to the brain. Phototransduction, from photon to nerve impulse, occurs in specialized photoreceptor cells in the outer retina. The human outer retina is enriched in rod photoreceptors in the periphery and cone photoreceptors in a central fovea (1). These two types of photoreceptors have been selectively specialized to perform phototransduction: light perception in high ambient light is mainly perceived by color-sensitive cone photoreceptors, whereas light perception in low ambient light is mainly perceived by rod photoreceptors (2, 3). Rods are very sensitive to light, in that a single photon can be detected within a rod photoreceptor through amplification of the signal via a G protein signaling process (1).

A rod or cone photoreceptor cell consists of four main regions: the outer segment, in which phototransduction occurs; the inner segment, in which protein and membrane synthesis occur; the cell body, in which the nucleus resides and where basic cellular functions occur; and the synaptic terminal, at which connections to bipolar and horizontal cells occur (4, 5) (Fig. 1). Rods and cones differ, however, in the shape of the outer segment and how the membrane of the outer segment is organized. Cone photoreceptors have cone-shaped outer segments that are shorter and wider than rod outer segments, whereas rods are longer and thinner, reaching through the outer retinal layer to contact

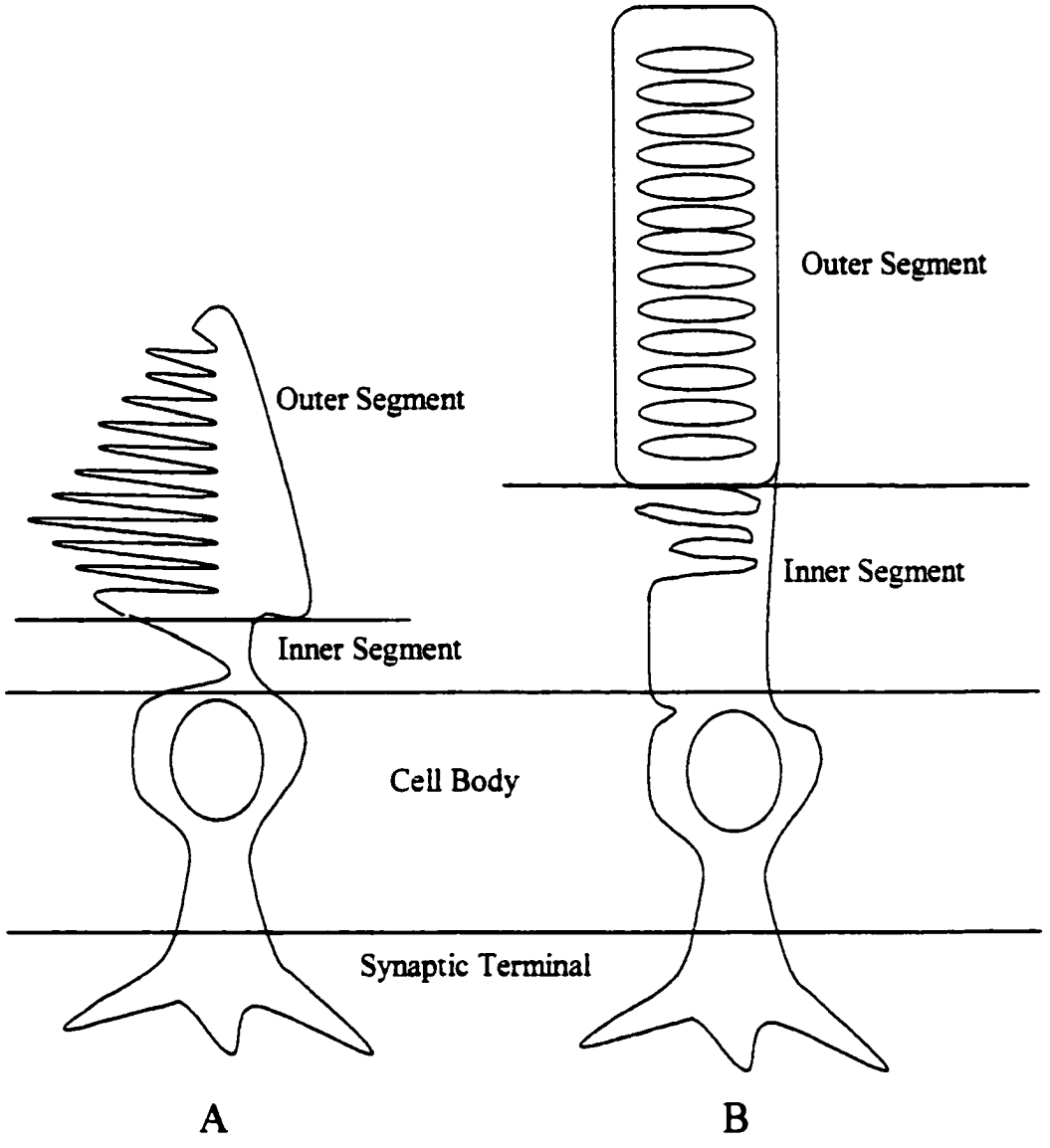

Fig. 1. Structure of cone and rod photoreceptors. The cone photoreceptor is comb-shaped with a single membrane comprising inner and outer membranes (*A*). The rod photoreceptor is rod-shaped and is comprised of two separate membrane systems: an outer plasma membrane and a system of inner disks (approximately 2000 per cell) (*B*). Both types of photoreceptor have four major sections: outer segment, inner segment, cell body, and synaptic terminal.

the retinal pigment epithelium (1, 5). The plasma membrane of a cone cell is continuous and does not form separate disk membranes as in rod cells (2). Thus, the cone plasma membrane resembles a comb-like structure in which a continuous membrane folds into layers to comprise the outer segment. The rod membrane system is dual: A single plasma membrane encloses several layers (approximately 2000 per cell in humans) of separate membranous disks (2, 5).

The phototransduction cascade has been studied more extensively in rods than in cones, because rod preparations are typically easier to separate from the rest of the retina because of the structure of the rod. The membrane disks of rods are synthesized at the boundary between outer and inner segments of the cell so that sections of plasma membrane continually evaginate to form small disks as proteins are inserted into the membrane at the boundary (1-3). This boundary is the thinnest point of the rod cell so that mechanical stress can cause the membrane to break, thus separating the rod outer segment from the rest of the retina. Preparations such as these have provided enriched outer segment cell extracts for study (2, 3).

The Phototransduction Cascade

The phototransduction cascade is dependent on several proteins that are expressed exclusively in the retina, some specific only to photoreceptor cells. The main enzymes involved in rod phototransduction are rhodopsin, transducin, and 3'-5' cyclic guanosine-monophosphate (cGMP) phosphodiesterase type VI (PDE6) (Fig. 2). PDE6 is the third enzyme in a series of cell signaling events that is initiated by rhodopsin.

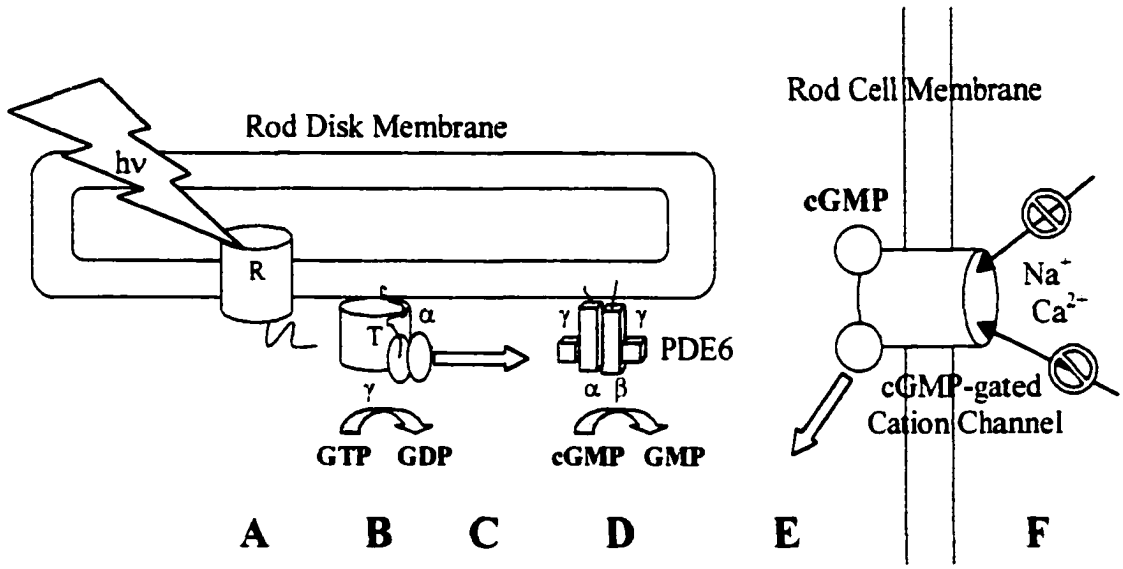

Fig. 2. The phototransduction cascade. A photon (hν) excites rhodopsin (R) through a photoisomerization event (*A*). Activated rhodopsin facilitates the exchange of GTP for transducin (T)-bound GDP (*B*). Activated transducin α subunit is released and interacts with rod phosphodiesterase (PDE6) to release inhibition by the γ subunits (*C*). Active PDE6 cleaves cGMP to GMP (*D*). Loss of cGMP within the cytoplasm causes cGMP to be released from the cGMP-gated channel (*E*), causing closure of the channel and exclusion of cations (*F*).

Rhodopsin—Rhodopsin is the most abundant of all rod photoreceptor proteins, accounting for 85% of the total protein in the outer segment of the photoreceptor cell (2). Rhodopsin is a seven-pass transmembrane protein that resides in both disk and cell membranes of the rod cell outer segment. Similar opsins are found in cone photoreceptors (blue, green, and red opsins), all encoded by separate genes with high homology (2). Rhodopsin complexed to the cofactor Vitamin A aldehyde (11-*cis*-retinal) is able to absorb light between 400 and 700 nm wavelengths and maximally at 500 nm (2). The cone opsins absorb maximally at 450 nm (blue), 530 nm (green), and 565 nm (yellow) (2). Photons are translated into chemical energy as 11-*cis*-retinal is isomerized (with six intermediate conformations) to all-*trans*-retinal, thus generating metarhodopsin I, a highly energetic compound (2). This change in the retinal cofactor causes a conformational change in rhodopsin, yielding its active form, metarhodopsin II (6). Rhodopsin remains active as long as all-*trans*-retinal is attached (nanoseconds) and can interact with the membrane-bound G protein, transducin (6). A single activated molecule of rhodopsin can interact with several molecules of transducin, thus amplifying the signal. When all-*trans*-retinal is removed, rhodopsin is inactive, returning to its original conformation, in which another molecule of 11-*cis*-retinal is covalently bound (2, 6).

Transducin—Rhodopsin activates transducin, a membrane-bound heterotrimeric G protein consisting of alpha, beta, and gamma subunits and the major G protein in rod photoreceptors (7). When active rhodopsin binds to the transducin trimer, it facilitates the exchange of a transducin-associated molecule of guanosine diphosphate for free guanosine triphosphate (GTP) on the alpha subunit (6). The exchange of nucleotides

causes a conformational change that promotes release of the transducin alpha subunit from the membrane-bound beta/gamma heterodimer as the active form of transducin (8). The free, activated transducin alpha subunit is then able to bind to PDE6 (9). Transducin alpha primarily interacts with PDE6 gamma subunit to remove an inhibitory constraint so that PDE6 becomes fully active (10, 11).

PDE6—Transducin with GTP bound activates PDE6, the holoenzyme consisting of four subunits: an 88-kDa alpha subunit, an 84-kDa beta subunit that is highly homologous (72%) to the alpha subunit, and two 11-kDa gamma subunits (9, 12-14). The alpha and beta subunits comprise the catalytic core of the enzyme: previous studies have revealed a PDE6 stoichiometry of alpha/beta/$(gamma)_2$ or $(alpha)_2/(gamma)_2$, but not $(beta)_2/(gamma)_2$ (9); however, alpha/beta/$(gamma)_2$ is considered the only physiologically relevant arrangement. The gamma subunits function normally as an inhibitory constraint: When transducin alpha associates with PDE6, the gamma subunits are displaced to fully activate the catalytic sites (9). The gamma subunits have also been shown to be necessary for proper folding of the holoenzyme (15). The alpha and beta subunits contain highly conserved sequences: The carboxy-terminal catalytic domain is comprised of amino acid residues 555 to 790 (16, 17), and the carboxy-terminal recognition site CXXX is used by the cell to signal post-translational prenylation and carboxymethylation for association with the cell membrane (18, 19). The PDE6 alpha subunit (PDE6A) is farnesylated, and the PDE6 beta subunit (PDE6B) is geranyl geranylated and is the major anchor for membrane association (18, 19). PDE6 activity has been shown to increase from approximately 50 mol of cGMP turned over per mol of protein to as much as 3700

mol of cGMP per mol of protein when activated by transducin (6). This rate of turnover corresponds to approximately a 10^6-fold difference of the light-stimulated activity compared with the dark-adapted basal activity (2). There are four cGMP binding sites within the PDE6 holoenzyme, including two sites within the amino-terminal region that are distinct from the catalytic sites (20). It is postulated that the binding of cGMP to these sites may regulate activity of the enzyme, as the enzyme is able to freely exchange two molecules of cGMP only in its inactive soluble form, compared with one in its active insoluble form (21). Furthermore. cGMP binding to noncatalytic sites may contribute to the association of the gamma subunit to the alpha/beta catalytic core, thus influencing regulation of the enzyme and intracellular cGMP levels (21).

Cyclic GMP as second messenger—PDE6 exclusively cleaves the nucleoside 3', 5'-cGMP to yield guanosine monophosphate (5'-GMP) (6). The second messenger cGMP is present in the photoreceptor cell in large quantities in order to bind to and open a nonselective cGMP-gated cation channel in the outer segment membrane in dark conditions (3, 6). The cGMP-gated channel mainly controls the amount of Na^+ and Ca^{2+} ions within the outer segment, working in combination with a Na/Ca-K exchanger in the outer segment membrane (3). The cGMP-gated channels generally remain open in the dark-adapted state so that Na^+ and Ca^{2+} ions flow freely into the cell in the presence of high cGMP levels (3). Ion flow out of the cell is accomplished by voltage-gated K^+ channels that allow K^+ to flow out of the inner segment, thus creating a dark current loop (3). The Na^+ and K^+ balance is mediated by a Na^+, K^+ ATPase in the inner segment membrane so that the Ca^{2+} concentration in the outer segment is kept at approximately

400 nM by the balance of influx through the cGMP-gated channel and efflux through the Na/Ca-K exchanger (3). In this balanced state, the cell is depolarized at approximately 40 mV and, as a result, releases the neurotransmitter glutamate at a constant rate at the synapse of the photoreceptor cell (3). The rod cell remains in this depolarized state until the balance of ions is upset by light induction (3).

When rhodopsin is activated by light, causing the subsequent activation of transducin then PDE6, cGMP levels change as the molecules are cleaved by active PDE6 (3). As intracellular cGMP levels fall, cGMP falls from its channel binding sites and the cGMP-gated ion channel closes (3). Loss of ion flow through the channel causes the rod cell to hyperpolarize as the ion potential difference across the membrane changes (1-3, 6). The hyperpolarity of the membrane is an electrochemical signal that is then sent via cell membrane to a synapse with bipolar nerve cells in the outer plexiform layer (1, 6). This signals the photoreceptor cell to inhibit glutamate release into the synapse (3). Intracellular Ca^{2+} levels also decrease as the Ca^{2+} is excluded by the cGMP-gated channels and constantly expelled via the Na/Ca-K exchanger in the outer segment membrane (3).

Simply stated, neural transduction consists of the nerve impulse manifested as inhibition of glutamate release traveling along the bipolar cell through the retina, where it synapses within the inner plexiform layer with ganglion cells (6). Horizontal and amacrine cells within the inner nuclear layer modify the signals sent by the photoreceptors to the ganglion cells (1). The ganglion cell axons comprise the optic nerve so that the nerve impulse then travels to the visual centers of the brain as neural input (6).

Recovery after phototransduction—Once the light stimulus is removed, photoexcitation ceases and the cascade system shuts down. The recovery process allows the cell to return to a depolarized state in which the photoreceptor is ready to respond again. The decrease in Ca^{2+} levels within the outer segment, resulting from the closing of the cGMP-gated channel and the constant efflux through the Na/Ca-K exchanger, stimulates the expression of the enzyme guanylate cyclase (22) through accessory proteins called guanylate cyclase-activating proteins (23, 24). Guanylate cyclase synthesizes cGMP from GTP to restore the cGMP level to that of preexcitation. The cascade is shut down through the inactivation of rhodopsin by phosphorylation and association with arrestin and through the inactivation of transducin and PDE6 by hydrolysis of the transducin α-associated GTP (3). As cGMP levels increase because of the activation of guanylate cyclase and the inactivation of PDE6, the cGMP-gated channels open and the cell returns to its depolarized state (3). Likewise, the rhodopsin cofactor retinal is also returned to its preexcitation state through a series of isomerization events that occur in the retinal pigment epithelium. Transducin α reassociates with its βγ membrane-bound core. Thus, the photoreceptor cell is ready to respond to light once again.

Transcription

In eukaryotic cell types, the basic mechanism of gene expression by RNA polymerase II-regulated promoters is similar: transcription factors bind within the 5' upstream region of a gene and promote the binding of the RNA polymerase II complex to the DNA so that transcription of heteronuclear RNA (hnRNA) may proceed (25). The hnRNA is then processed within the nucleus by capping the 5' end of the molecule, splicing out

introns, and adding a stabilizing poly-adenylate tail (25). This mature mRNA is able to leave the nucleus to travel to the cytoplasm where ribosomes translate mature mRNA into protein (25). It is often the number of times that transcription is initiated at the promoter that governs the amount of transcript and, thus, protein (26).

Control of expression of cell-specific genes may occur at any of the levels involved in transcription or translation; however, it is most often controlled at the level of transcription initiation, namely with transcription factor and/or repressor molecule binding (27). Transcription factors and repressor molecules both bind to DNA (sometimes through the association of another protein molecule) at specific sequences, called *cis*-binding sites, that are complementary to a DNA-binding region of the regulatory molecule (26). For instance, many DNA-binding transcription factors contain motifs such as alpha helices that are able to fit within the major or minor groove of the double helix so that amino acid side chains can interact with a specific base sequence within the DNA (27).

Many genes contain *cis*-binding sites for general transcription factors; that is, "housekeeping" genes that are constitutively expressed by RNA polymerase II usually contain a TATA box (named because the sequence of thymine-adenine-thymine-adenine is conserved) approximately 25 bases from the transcription start point (tsp, +1) where the general transcription factor TATA-binding protein binds (26). General transcription factors (for example, TATA-binding protein) that are available in all cell types are able to bind to the region near and/or the TATA box and promote constant levels of transcription (25). A constant level of (constitutive) transcription is necessary for housekeeping genes that encode proteins involved in basic cellular functions such as enzymes used in glyco-

lysis. However, many genes are not expressed in all cell types, and some of these genes do not contain a TATA box in the upstream promoter (26). Other *cis* elements have been discovered that are present in these regulated genes that promote RNA polymerase II binding through the binding of other transcription factors to a single (such as the Inr), or several, *cis* elements (26).

A promoter may also have another type of *cis* element, called a repressor molecule binding site, in which a specific molecule binds to prevent the promotion of RNA polymerase II to the tsp (26, 27). A repressor can work at a distance by changing chromatin structure or can work within the promoter to compete for binding sites, to sterically hinder the RNA polymerase binding site, or to bind to transcription factors without binding DNA and render them nonfunctional (27).

A promoter may have one *cis* element, transcription factor or repressor, or several in different combinations (25-27). Therefore, the genes that contain binding sites for specific transcription factors will be upregulated in those cell types that also contain that specific transcription factor (27). Likewise, genes containing repressor molecule binding sites will be upregulated in those cells that do not contain that specific repressor molecule (27). The different combinations of repressors and/or transcription factors allow for great diversity of transcription efficiencies in specific cell environments (25, 27).

Retina-Specific Transcription

The cells of the retina differ from other cells in the types and amounts of proteins that are expressed. There are proteins that are common to all retinal cells, as well as proteins that are common only to photoreceptors and, more specifically, to rod photore-

ceptors. The regulation of expression of these proteins is generally at the level of transcription so that a cell phenotype is dependent on cell-specific initiation of transcription (26). Several transcription factors have been shown to be retina-specific, in that they are expressed exclusively in retinal cells (although some are expressed in the pineal gland) and bind to promoters of genes that are expressed primarily in the retina (27). Fig. 3 shows a comparison of proximal promoter regions of some retina-specific genes. Some of the retina-specific transcription factors are important during development of retinal cells such as Pax6, Rx, and Erx (28). CRX and NRL are expressed developmentally and in adult retina as well (28, 29).

The *cis*-binding sites for many of the retina-specific transcription factors have been identified as shown in Table 1. Several retinal genes such as rhodopsin, PDE6A, PDE6B, arrestin, and IRBP have been shown to have one or more of these sites in the promoter region as deduced from the DNA sequence (7, 30-35) (Fig. 3). Functional studies in some genes have demonstrated binding of the transcription factors to these *cis* sites as well (36-42).

Retinal Transcription Factors

Cone rod homeobox factor (CRX) is a member of the Otx-like homeobox protein family, which act as regulators of gene expression during development. The *Crx* gene encodes a 299-amino acid protein that is expressed primarily in photoreceptors, but is also expressed in the pineal gland (47). The CRX protein is a transactivator that binds to different sites within promoters of photoreceptor-specific genes, including Ret-1, Ret-4, BAT-1, and CBE sites (48). These sites are present in the promoters of photoreceptor-

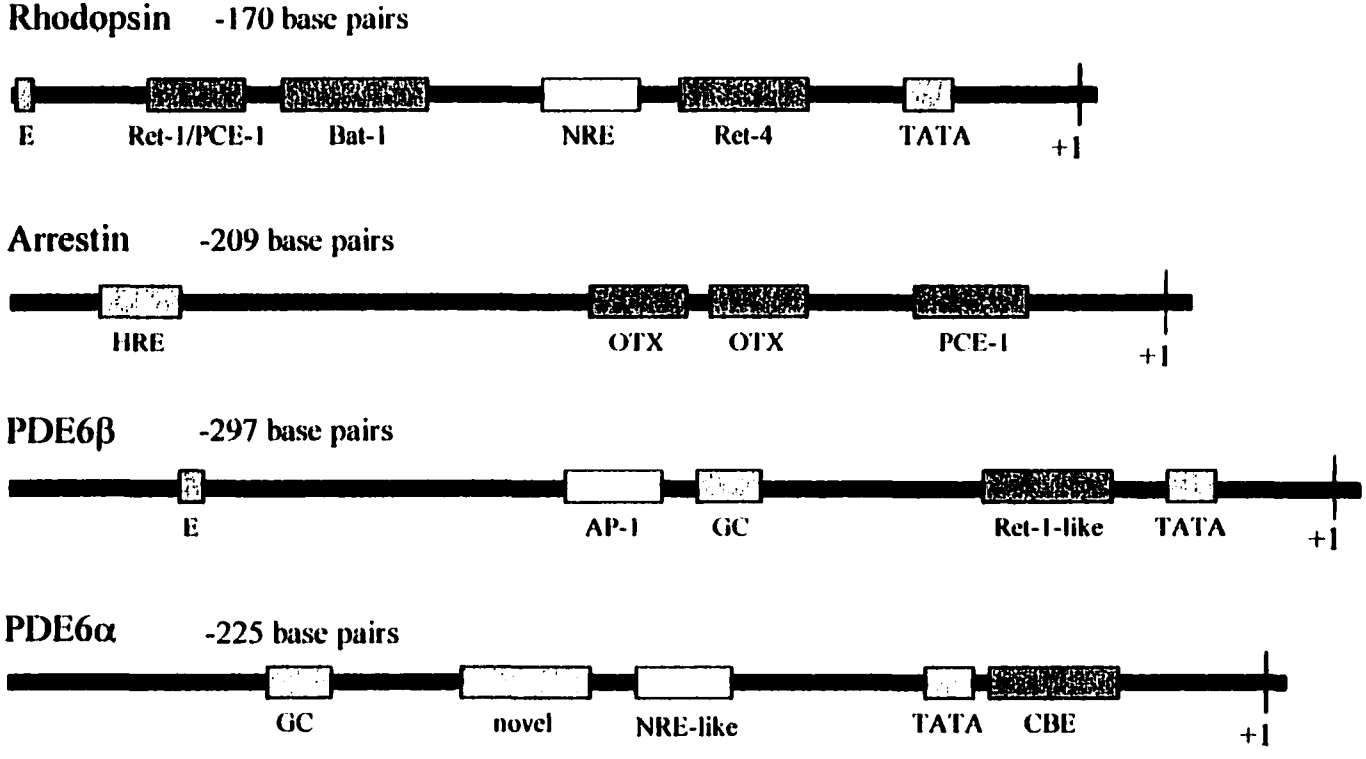

Fig. 3. Comparison of proximal promoter regions in known retina-specific genes. The proximal promoters are shown for rhodopsin, arrestin, PDE beta subunit, and PDE alpha subunit. *Boxes* represent putative binding sites for the indicated transcription factor. *White boxes* represent sites that bind NRL. *Dark gray boxes* represent sites that bind CRX. Promoter length that has been determined to direct photoreceptor-specific expression in transgenic mice is shown in base pairs.

Table 1.
Transcription factor binding sites and consensus sequences.

Transcription factor	Binding site	Consensus sequence[a]	Ref.
Pax-6	Ret-1/PCE-1	GTTAAT	43
Rx	Ret-1/PCE-1	GTTAATC	43
Erx	Ret-1/PCE-1	GTTAATC	43
Otx	Otx	ACTAATC	44
CRX	Otx	CCTAAT	44
CRX	CRXE	CTAATT	30
CRX	CBE[c]	C/TTAATC/T	29
c-jun/c-fos	AP1	TGACTCA	45
CREB[b]	CRE[d]	TGAGCTCA	45
NRL	NRE[e]	$TGAN_{6-8}GCA$	46

[a]Sequence shown is antisense strand.
[b]CREB, cAMP response element binding protein.
[c]CBE, CRX binding element; CRE, CREB response element; NRE, NRL response element.

specific genes encoding PDE6B, arrestin, rhodopsin, interphotoreceptor retinoid-binding protein (IRBP), and the cone opsins (32-36, 39, 49, 50-54). The CRX consensus binding site was identified by Chen and colleagues using DNA footprinting studies as C/TTAA TCC, similar to binding sites of other Otx-like and homeodomain proteins in which a lysine residue is at position 51 in the homeodomain (36). It has been suggested that CRX is involved in development of photoreceptor cells, both rods and cones, during a phase where specification of the cell occurs (28). The expression of CRX within a developing postmitotic multipotent cell then determines the fate of the cell to become a precursor of retinal cells (28). Further, it is thought that cells specified via CRX expression can be further specialized into bipolar cells without continued activation by CRX or into mature rod cells with continued activation by CRX (55). CRX has also been shown to be present in adult photoreceptors (28). Co-expression of CRX and a photoreceptor gene promoter reporter construct in non-retinal cells showed an increase in luciferase activity, including

a 6.5-fold increase for the rhodopsin promoter, a 4.5-fold increase for the IRBP promoter, a 2.5-fold increase for the PDE6B promoter, and a 2-fold increase for the arrestin promoter (36).

A transgenic model of a CRX dominant-negative allele in the mouse has shown that CRX transcript segregates to the outer nuclear layer of the retina, but proper formation of outer segments of photoreceptors does not occur. This finding confirms the specific developmental transcription of CRX because the mutant allele was transcribed, and confirms its role in proper outer segment formation because the mutant protein inhibited normal development and resulted in a CRX deficiency (56). However, a transgenic mouse in which the entire CRX gene has been knocked out has shown that retinal development occurs; but, at postnatal days 12-14 when outer segments should be fully formed, the photoreceptors begin to degenerate (57). This implies that other genes, for instance, other members of the Otx family, are able to partially compensate for the absence of CRX, although the continued absence past development is deleterious (57). This is consistent with the dominant-negative transgenic mouse model in that the CRX mutant allele was competitively binding to promoters and not transactivating, whereas the absence of any CRX allele allowed the cell to compensate in development by using another similar transcription factor.

Furthermore, mutations have been discovered in the CRX gene that lead to at least three human diseases, Leber congenital amaurosis, autosomal dominant retinitis pigmentosa, and autosomal dominant cone-rod dystrophy type 2 (58, 59). Cone-rod dystrophy and retinitis pigmentosa are degenerative diseases, with progressive vision loss

beginning after retinal development has occurred initially (59). Leber congenital amaurosis is more severe, often causing total retinal blindness at birth (58).

Neural retina leucine (NRL) zipper protein is a basic zipper protein in the bZIP family shown to dimerize as a homodimer and as a heterodimer with other bZIP proteins (60). Dimers of bZIP factors bind to the NRL response element (NRE) consensus sequence $TGCN_{6-8}GCA$, where the internal bases are similar to the AP1 site (TGACTCA) or the cAMP response element (TGAGCTCA) (46). It has been shown that NRL binds to a conserved NRE site in the rhodopsin proximal promoter to positively regulate expression (46). It has also been shown that NRL is expressed at continuous high levels in the adult retina (46). Furthermore, addition of a naturally occurring truncated form of NRL that is lacking the DNA-binding region is able to dominantly and negatively regulate expression, presumably by binding normal NRL through its leucine zipper and preventing proper alignment with the DNA helix (46).

It has been shown that CRX transactivation works synergistically with NRL transactivation to produce a several-fold increase in expression of a rhodopsin promoter/luciferase reporter gene construct (36). Co-expression studies *in vitro* showed a synergistic effect on rhodopsin expression when both NRL and CRX were expressed, signified by a 115-fold increase in luciferase reporter activity compared with a 6.5-fold increase in luciferase activity with CRX alone or with a 3-fold increase with NRL alone (36, 48). A possible mechanism of this synergism has been explained as a physical interaction of CRX and NRL, as the NRE and Ret-4 sites within rhodopsin are adjacent within the proximal promoter: CRX may recruit NRL to the site, or vice versa (61) (Fig. 3). It was suggested through yeast two-hybrid assays that the leucine zipper of NRL is able to

interact with CRX, and deletion analysis showed that the homeodomain of CRX is responsible for this interaction (61). Conversely, deletion analysis showed that the leucine zipper of NRL was essential for the interaction (61).

Rod Photoreceptor-Specific Promoter Studies

The most studied photoreceptor-specific promoter is the rhodopsin promoter, which serves as a model for promoters of other photoreceptor-specific genes. Sequence analysis of the upstream region to –2 kilobase pairs has revealed two distinct promoter regions, namely the rhodopsin proximal promoter region (RPPR), located –176 to +70 base pairs relative to the mRNA start site, and the rhodopsin enhancer region (RER), located approximately 1.5 to 2 kilobase pairs upstream (62-64). Within the RPPR are several *cis*-acting DNA regulatory elements detected by electrophoretic mobility shift assay and DNase I footprinting: Ret-1/PCE-1, Ret-2, Ret-3, Ret-4, Mash-1, Bat-1, and NRE sites (35, 37, 42, 48, 49, 65) (Fig. 3). It has been shown that Ret-1/PCE-1, Ret-4, and Bat-1 *cis* elements respond to the transcription factor CRX, whereas NRE responds to the transcription factor NRL (36, 47, 48). CRX has been shown to bind other retina-specific gene promoters at Ret-1/PCE-1 sites, such as arrestin and IRBP (66, 67).

The coding region of human PDE6A spans approximately 100 kilobase pairs on chromosome 4 and consists of 22 exons and corresponding introns, with a 1.9-kb 3' untranslated region present in mRNA (30). The 5' untranslated region was determined by ribonuclease protection assay, which predicted a tsp 120 nucleotides upstream of the initiator methionine ATG codon (30). A second minor tsp was also found 140 nucleotides upstream of the ATG (30). To determine elements within the PDE6A promoter,

approximately 3.6 kilobase pairs upstream of the major tsp were sequenced and compared to known DNA segments, including repetitive elements and transcription factor binding sites (30). Seven separate repetitive elements were found in the upstream region including two Alu segments, and a partial Alu segment (30). In the proximal promoter region, transcription factor binding sites include CBE (-34 to -44), TATA-like (-46 to -52), NRE-like (-72 to -82), a novel site conserved in mouse and human (-84 to -94), and SP1 (-100 to -105) sites (30) (Figs. 3, 4). The CBE and TATA-like sites were shown to bind retinal extract-specific proteins in a DNA footprinting experiment (30). The CBE *cis* element is a CRX binding element, although in opposite orientation (CTTAATC), that has been shown to bind the transcription factor CRX in rhodopsin (29, 30, 35).

The promoter of PDE6B has also been cloned and is similar in structure to the PDE6A promoter. There are two start sites within the PDE6B gene as in PDE6A, at positions +1 and +32, and it has been suggested that alternate transcripts are possible (31). Within the 5' upstream region extending to –1.4 kilobase pairs, there are several *cis* regulatory elements (31). A TATA-like box (-25 to -31), a CAAT-like box (-868 to -873), two SP1 sites (-51 to -56, and -824 to -829), an AP1 site (-64 to -69), and a Ret-1/PCE-1 site (-36 to -41) were found within the upstream region (31) (Fig. 3). Transient transfection in the Y79 retinoblastoma cell line has shown that an ~90-bp segment upstream of the tsp is capable of directing promoter activity (68). DiPolo and colleagues have demonstrated proximal promoter activity in cell culture that can be upregulated by cotransfection of NRL and CRX (68). Furthermore, Ogueta and colleagues showed that a short fragment (350 base pairs, including a Ret-1 site) of the PDE6B promoter was capable of directing expression of a reporter gene in transgenic mice (69). Expression of

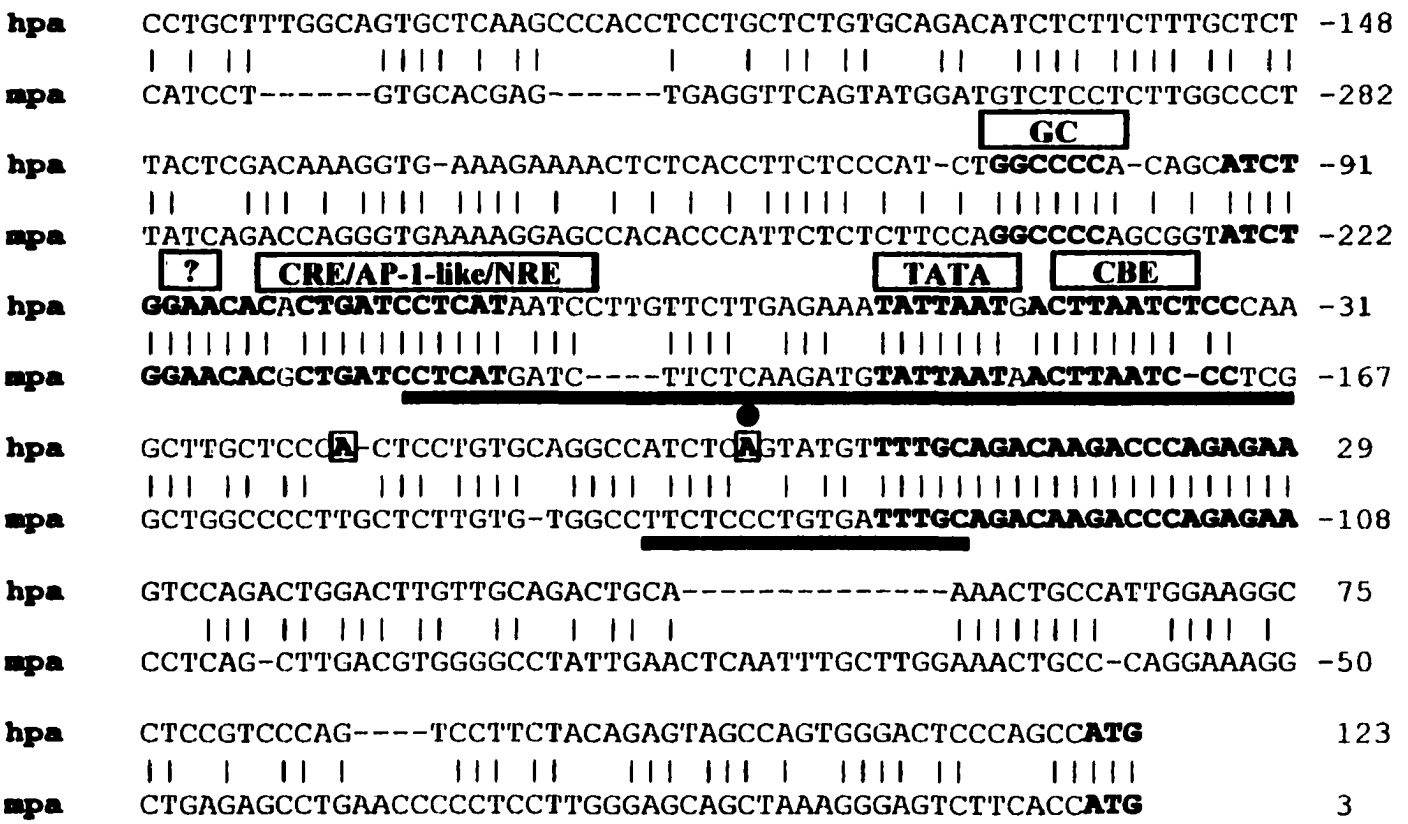

Fig. 4. Sequence of the PDE6A proximal promoter region. The human sequence (hpa) is compared to the mouse sequence (mpa). Homology is indicated by the *lines* between conserved bases. Putative transcription factor binding sites are indicated above the sequence in *boxes*. A novel conserved site is denoted as ?. The major transcription start point is marked by a *large dot* above. The major and minor transcription start points are indicated by a *box around the base letter*. *Black bars* below sequence indicate regions of footprinting with CRX. The initiator methionine codon (ATG) is indicated in *bold type*. Highly conserved regions are also indicated in *bold type*.

the transgene was shown to be limited to the outer retina (69). A recent study using a PDE6B promoter construct in a Y79 human retinoblastoma cell culture showed through mutation analysis that the AP1 site was essential to maximum expression of a reporter gene (68).

RATIONALE

The purpose of this study was to characterize the proximal promoter region of the human rod photoreceptor cGMP phosphodiesterase alpha subunit gene and show that this promoter confers tissue-specific expression. This was to be accomplished in three specific aims. The first specific aim tested the necessity of the specific transcription factor CRX in the expression of PDE6A in *Crx-/-* mice. The second specific aim examined the specificity of the transcription factors CRX and NRL for the PDE6A promoter in two ways: first, by determining their effect on PDE6A promoter driven expression of reporter gene in a heterologous cell system and, second, by examining the binding potential of CRX and NRL to specific oligonucleotides in electrophoretic mobility shift assays. The third specific aim tested the sufficiency and specificity of the PDE6A minimal promoter to direct tissue-specific expression in transgenic mice.

Specific Aim 1

CRX is a member of a large family of homeobox transcription factors, and other members of the family have been suggested to regulate transcription in the absence of CRX. Cross-reactivity, or non-specific binding of transcription factors, within a family is generally accepted, although the binding affinity and/or function may differ slightly from one family member to another (26). Thus, we investigated whether PDE6A is transcribed in the absence of CRX in the *Crx-/-* (knockout model) mouse and the extent of the difference in transcription of PDE6A when CRX is absent, compared to normal mice.

Specific Aim 1 was to determine the necessity of the transcription factor CRX in the expression of rod PDE6A by quantifying approximate PDE6A mRNA levels in *Crx-/-* mice. This was accomplished by examining steady-state levels of PDE6A mRNA in *Crx-/-* mouse retinas with reverse transcription polymerase chain reaction (RT-PCR), and by comparing levels of PDE6A mRNA in *Crx-/-* and normal mouse retinas compared to an internal control in semi-quantitative RT-PCR.

The first goal of this aim was accomplished by RT-PCR methods, using RNA extracted from retinas of 10-day-old mice, a developmental period when the retinas are nearly developed and still intact in the CRX knockout model (57). Total RNA, which would include transcripts of all genes being expressed at this developmental stage, was extracted from pooled samples of the 10-day-old mouse retinas. First-strand cDNA was synthesized using reverse transcriptase. Amplification of cDNA by PCR was accomplished using primers specific to mouse cDNA for the genes *Pde6a*, *Pde6b*, rhodopsin, and *Crx*. RT-PCR can be semi-quantitative, meaning that the amount of product generated is proportional to the initial amount of specific transcript, as long as the amplification step remains in the linear range. That is, if a specific transcript is rare, the amount of PCR product is low; however, if a transcript is abundant, the amount of PCR product is high. Quantitation of mRNA using this method also relies on the use of a standard internal control, which is used to normalize starting amounts of cDNA template. For instance, the ubiquitous cellular enzyme glyceraldehyde-3-phosphate dehydrogenase (GAPDH) can be used as a standard to determine the relative amounts of a specific transcript because GAPDH is known to be transcribed at a high stable rate and, thus, produces large quantities of mRNA.

The second goal of Aim 1 was also accomplished by RT-PCR in which quantitation is possible. The same cDNA samples used in the first goal of Aim 1 were amplified to 25 cycles, which was determined to be within the linear range of amplification for each of the primer sets (data not shown). All amplification reactions originated from the same cocktail to control for reagent volumes. For example, a major cocktail was made containing buffer, water, deoxynucleotides, and DNA polymerase. This cocktail was then divided into minor cocktails, and five volumes of cDNA was added, one volume for each of the primer sets. Each minor cocktail was then aliquoted into PCR thin-wall tubes. Appropriate primer dilutions were then added to each aliquot. Amplification was carried out according to the optimal temperature for each primer set. PCR products were separated on acrylamide gels, stained with ethidium bromide, and scanned on the Typhoon 8600 imaging system. The Typhoon system is very sensitive to fluorescent stains such as ethidium bromide, so very small amounts of PCR product could be visualized. PCR products for each cDNA sample (i.e., products of different primer sets using the same template) were run on the same gel and stained to standardize gel conditions. Band intensity was compared directly within a gel using Image Quant software. Thus, it is possible to interpret a quantitative difference in intensity of fluorescent signal as a difference in PCR product and, thus, as a difference in original transcript.

Specific Aim 2

Specific Aim 2 was to demonstrate the specificity of binding of transcription factors CRX and NRL to the rod PDE6A promoter *in vitro*. This was accomplished in two main goals: determining the effects of CRX and NRL on normal and mutant PDE6A

minimal promoter driven transcription through transient transfection assays, and demonstrating specific binding of CRX and NRL to specific normal and mutant PDE6A promoter fragment oligonucleotides through EMSA. The first goal examined the effect of CRX or NRL on the minimal promoter, the effect of CRX and NRL on the minimal promoter, and the effect of CRX and NRL on mutant minimal promoters. The second goal examined the binding of CRX or NRL to site-specific double-stranded oligonucleotides, and competition in binding of selected oligonucleotides to CRX and NRL.

In the first goal, comparisons of results from transfection experiments were 1) among plasmids containing different lengths of promoter fragments (that is 260-bp, 300-bp, and 1060-bp fragments); 2) among the addition of CRX or NRL or both together; and 3) among the mutation of two putative CRX binding sites. These experiments were accomplished using a heterologous system, in which several plasmids are cotransfected into cells to express all proteins required for each experiment. For instance, plasmids containing the Renilla luciferase (used as an internal control), the promoter construct in front of the firefly luciferase reporter gene, and the genes for CRX and/or NRL with constitutive promoters were all transfected in the same experiment.

In order to show the tissue specificity of the PDE6A promoter, the promoter fragment was attached to a reporter gene and the construct was introduced into a non-retina cell line. The human embryonic kidney (HEK 293) cell line was used for this purpose. The HEK 293 cell line is derived from embryonic kidney stem cells and, thus, is an immortal cell line. Because it is not neural in origin, it is believed to be very distinct from retinal cells. Thus, it is possible to show the effect of single or multiple transcription factors on a promoter by adding each factor individually to the heterologous

tissue culture system. For instance, to test the effect of CRX on the PDE6A promoter, both the PDE6A promoter driving expression of luciferase and a strong SV40 promoter driving CRX expression were cotransfected into the HEK 293 cells. The effectiveness of CRX in promoting transcription of PDE6A could then be shown by the amount of luciferase activity that resulted from the transactivation.

Constructs used in the experiments contained 260, 300, and 1060 base pairs surrounding the transcription start point of the PDE6A promoter driving expression of firefly luciferase (Fig. 5). Firefly luciferase is an easily detectable reporter protein that gives a rapid signal, and subattomole quantities can be detected through the strong luminance signal. Other constructs used in experiments contained transcription factor genes CRX or NRL, both driven by the strong SV40 promoter. and either internal control reporter genes β-galactosidase, driven by the strong SV40 promoter, or Renilla luciferase, driven by the strong CMV promoter. PDE6A promoter constructs were also mutated to discern the importance of two adjacent regions within the promoter where CRX has been shown to bind in DNA footprinting studies (Fig. 6). Mutated constructs contained the 300-bp PDE6A promoter construct as above, with one of two possible CRX-binding sites altered (Fig. 7).

The two transcription factors CRX and NRL, which have both been shown to direct photoreceptor-specific transcription in other genes, were tested in cotransfection experiments to determine their effects both singly and together on different PDE6A promoter constructs. Because a CBE site has been shown in the promoter of PDE6A, we expected that there would be a large effect resulting from CRX transactivation. It was

Fig. 5. Comparison of PDE6A promoter constructs used in transfection studies. The indicated segments are contained in the promoterless plasmid pGL3, a firefly luciferase reporter plasmid. Transcription factor binding sites are shown as *boxes* with names given only on the first construct. *Dark gray bars* above constructs indicate CRX-footprinted regions (Fig. 6). *Light gray bars* above constructs indicate DNase I-footprinted regions. *TSP*, transcription start point; *bent arrow*, translation start point; *Luc*, firefly luciferase gene. *White boxes* in the pGL3-M13 and pGL3-M16 plasmids indicate mutated binding sites.

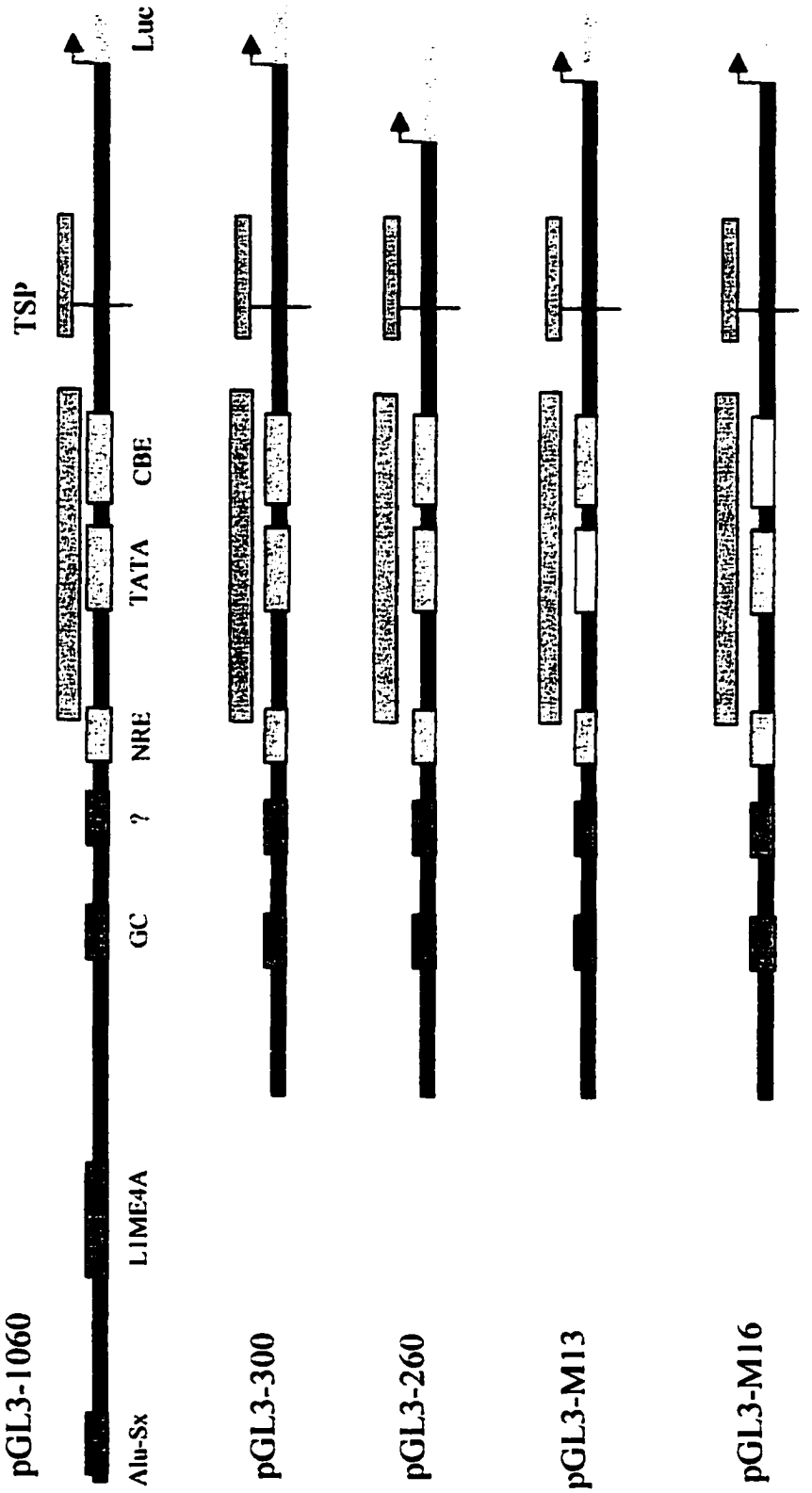

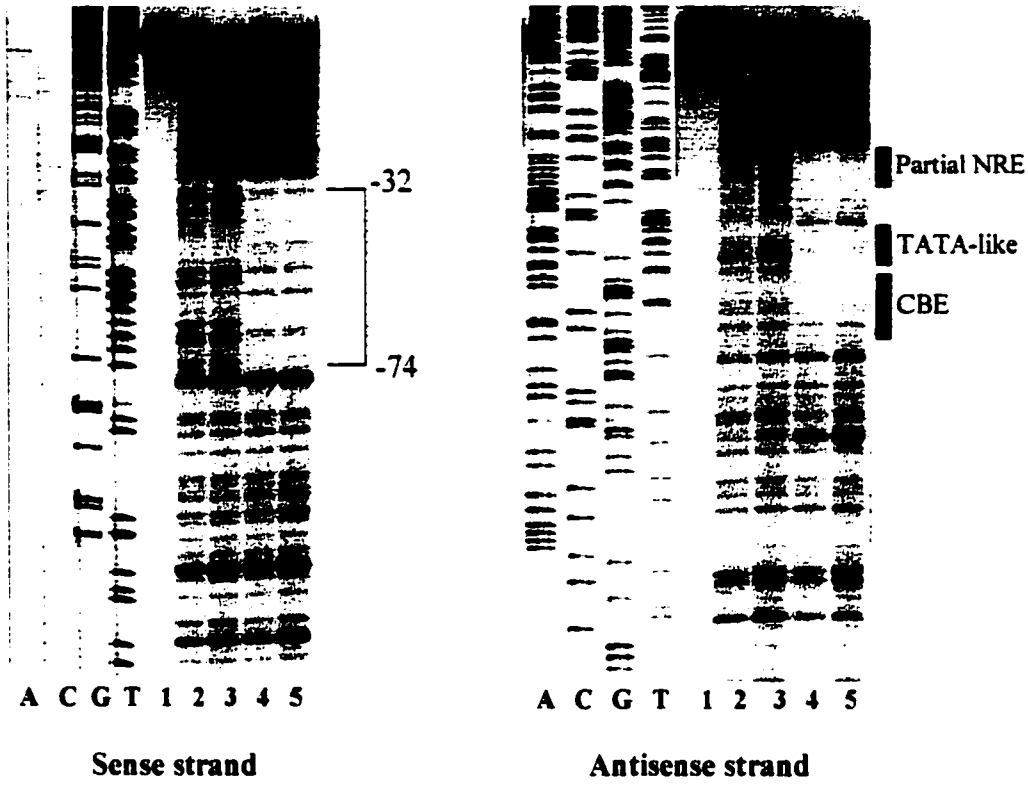

Fig. 6. CRX footprinting of the PDE6A promoter. CRX protein protected the indicated regions from DNase I digestion. Region marked represents the –32 to –74 region within the promoter that encompasses the CBE, TATA-like, and partial NRE-like sites. *Lane 1*, no DNase I; *lanes 2* and *3*, no protein; *lanes 4* and *5*, truncated CRX homeodomain protein added. Data from unpublished results of Drs. Shiming Chen and Don Zack.

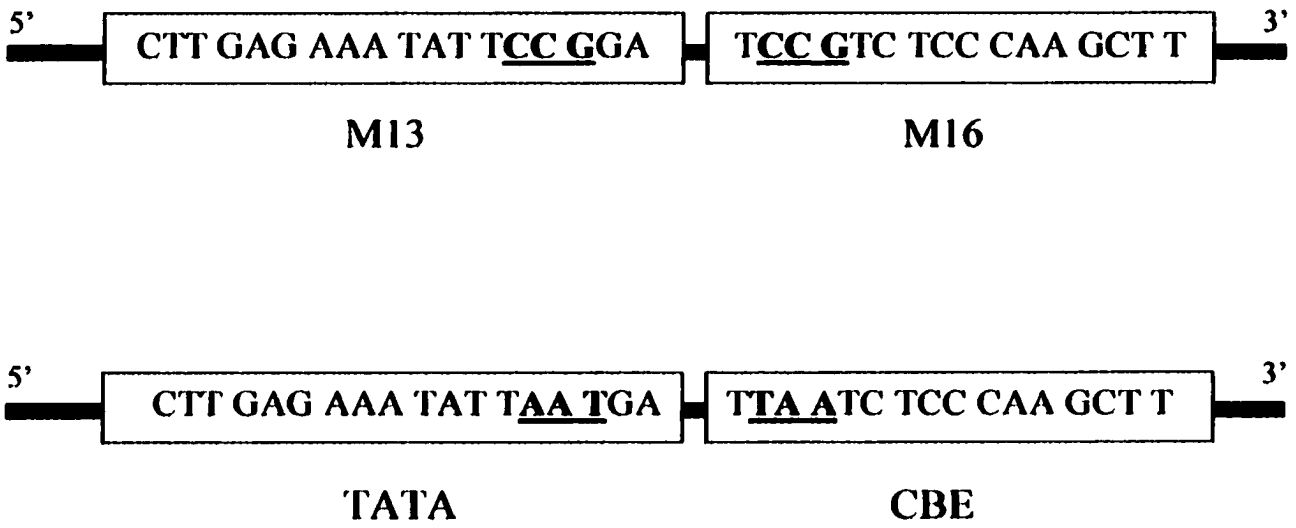

Fig. 7. Mutations generated in the pGL3-300 plasmid. Mutations were generated using long oligonucleotides containing the DNA sequence changes and then amplified by PCR. Mutations were designed to create a substitution within the CBE and TATA binding sites to remove the internal TAA and replace it with CGG. Mutated bases are *underlined in bold type*.

proposed that a conserved region of the PDE6A promoter (NRE-like) might bind NRL, so we also expected an effect resulting from NRL transactivation. Synergism between CRX and NRL was also investigated in the PDE6A gene because synergism between CRX and NRL was reported previously in the rhodopsin promoter (36).

The second goal, EMSA, was accomplished using the purified protein NRL and partially purified CRX with oligonucleotides representing the CBE, TATA-like, and NRE-like sites within the PDE6A promoter. The EMSA method determines specific binding of a protein to an oligonucleotide (that is, a short, double-stranded piece of DNA) containing the sequence of interest. A specific oligonucleotide of known sequence is 5' labeled with γ-^{32}P-ATP and mixed with protein. When separated by polyacrylamide gel electrophoresis, unbound oligonucleotide will migrate through the gel at a faster rate than oligonucleotide bound to protein. thus creating the shift in gel mobility. Mobility shifts were determined using differing combinations of protein and oligonucleotide to show binding of protein to the DNA. Specific binding was determined by competition assays in which unlabeled oligonucleotide was added to a reaction to show that the unlabeled oligonucleotide was also able to bind the protein, thus competing away the labeled oligonucleotide. Self-competition studies showed the specificity of the oligonucleotide for the protein: if the protein is specific for the oligonucleotide, then equal parts of labeled and unlabeled oligonucleotide will produce a signal of approximately half the intensity of labeled alone. Likewise, any ratio of labeled to unlabeled oligonucleotide would show the same ratio in signal intensity.

The relative importance of the TATA and CBE sites was investigated through mutant oligonucleotides in which one (M16/TATA, CBE/M13) or both (M16/M13) sites

were mutated. Competition assays between each of the mutant oligonucleotides and against the normal CBE/TATA oligo nucleotide were performed to determine relative strength of promoter sites. If an unlabeled oligonucleotide was able to compete away labeled oligonucleotide rapidly and completely, then it can be proposed that the normal site of the competitor is stronger than the normal site represented by the complementary mutant. For instance, if CBE/M13 were able to rapidly and completely compete away CRX from labeled M16/TATA, this would indicate that CRX binding to the CBE site is stronger than CRX binding to the TATA site because the CBE of CBE/M13 is responsible for the competition. The locations of the oligonucleotides used in the EMSA experiments are shown in Fig. 8.

Specific Aim 3

The goal of this aim was to determine the sufficiency and specificity of the rod PDE6A minimal promoter to direct tissue-specific expression of the bacterial β-galactosidase reporter gene in transgenic mice. This goal was accomplished by generating a transgene construct for a -200 to +101 (300 base pairs) upstream fragment of the promoter, performing RT-PCR to analyze transgene transcription, and performing *in situ* hybridization to localize transgene-specific mRNA within the retina.

A construct containing approximately 300 base pairs surrounding the transcription start point of PDE6A was prepared for microinjection into mouse embryos (Fig. 9). The promoter fragment was ligated to the reporter gene bacterial β-galactosidase that was attached to a mouse protamine region containing a polyadenylation site and a 3' intron. The purpose of the polyadenylation site was to provide a signal for polyadenylation,

Fig. 8. Location of EMSA oligonucleotides. Sequence of oligonucleotide is shown *boxed* for NRE, TATA, and CBE oligos. M13 and M16 oligos differ only in sequence as shown in Fig. 5. Oligonucleotides CBE/TATA and CBE/TATA/NRE are represented by *boxes* that span the sequence above. M16/M13 oligo contains mutations in both sites as in Fig. 5. CBE/TATA/AP1 oligo contains a mutation that converts the NRE site to a true AP1 site, TGACTCA, by deleting the dinucleotide TC (bases –78 and –77). The transcription start point and initiator methionine codon are in *bold*.

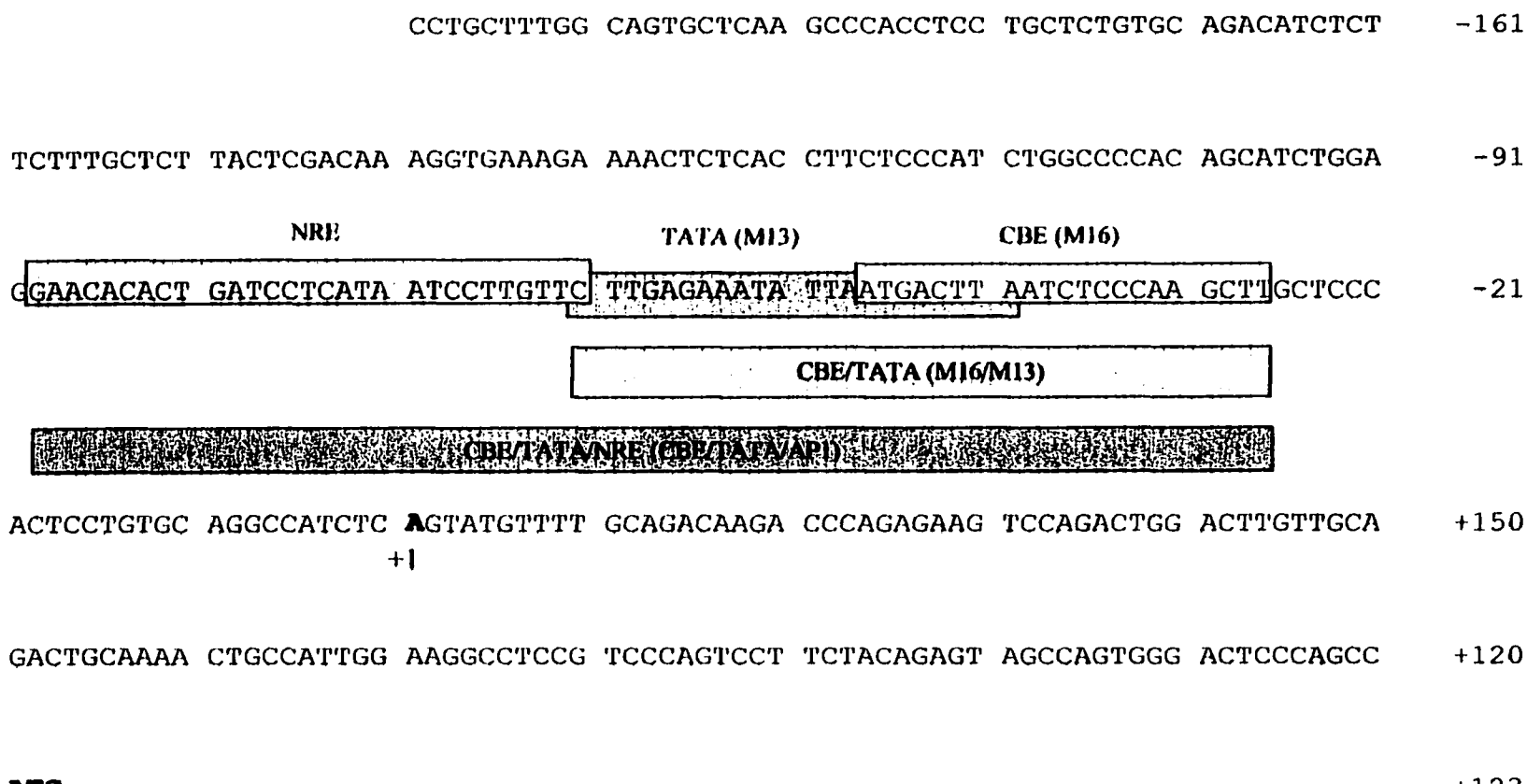

which is essential to the stability of RNA transcript (25). The 3' intron was included so that the transcript would be processed into mRNA: in eukaryotes, splicing of pre-mRNA is essential so that receptors on the nuclear pores recognize it and allow the mature mRNA to leave the nucleus to be translated into protein (25). The *rd* allele, which causes an autosomal recessive retinal degeneration phenotype common in many mouse strains, was present heterozygously in the ova used for microinjection; mice were bred to exclude the *rd* phenotype (70). Tail samples were collected and digested to extract genomic DNA, and mice were screened by PCR to determine presence of transgene. Mice positive for the transgene and negative for *rd* phenotype were bred, sacrificed, and studied. It was determined that the reporter gene was not expressed in these mice. Therefore, it was necessary to confirm that the transgene was being transcribed: RT-PCR confirmed that transcript was present in all lines. In order to determine the spatial distribution of transcript within the mouse retina, *in situ* hybridization was performed using probes specific to the transcript. The probes used were generated with cDNA of transgenic mouse retina and were specific for sense (experimental negative control) and antisense (experimental) of transgenic transcript, and sense (negative control) and antisense (positive control) of the PDE6 β subunit transcript used as a photoreceptor-specific control. Hybridization and detection of PDE6B antisense probe localizes the area of retina where the transgene should be expressed. Hybridization and detection of either sense probe should show only background staining because the sequence is identical to the transcript and not complementary and, so, it should not bind. Hybridization and detection of the transgene antisense probe localizes the transgene.

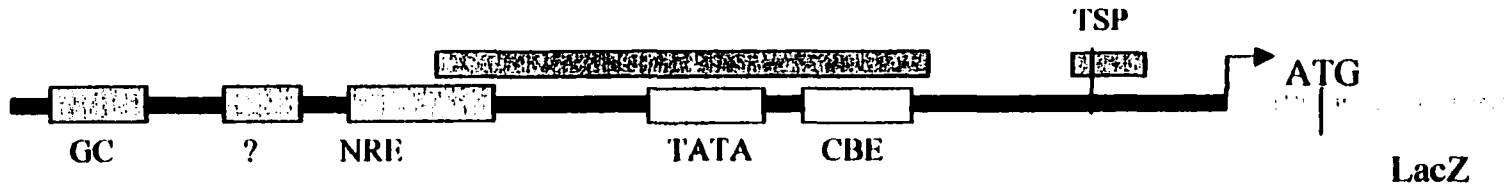

Fig. 9. Construct of fragment used to generate transgenic mice. The construct shown was used for microinjection into C57/SJL hybrid embryos. *Blocks* denote putative transcription factor binding sites within the PDE6A promoter region. *LacZ* denotes the bacterial β-galactosidase gene used as a reporter. *TSP* denotes the primary transcription start point. A *bent arrow* denotes the translation start point. *ATG* denotes a second, out-of-frame initiator methionine codon. *Dark gray bars* above diagram denote CRX footprinted regions.

MATERIALS AND METHODS

Specific Aim 1

Extraction of RNA from mouse retinas—Mice (*Crx-/-*) obtained from Dr. C. Cepko, Harvard Medical School, were genotyped for the absence of the native *Crx* gene using PCR of genomic DNA (primer pair mCRX-f/mCRX-r, Table 2). Mice were inbred to obtain enough retinal tissue for study (approximately 100 mice). Pups were sacrificed at postnatal day 10 or 11, when retinas were known to appear about the same as in normal littermates (29). Mice at 10-11, 45, and >60 days were sacrificed, and the retinas were removed and quick frozen in either liquid nitrogen or a dry ice/ethanol bath, then stored at –80 °C until further use. Retinas were pooled into groups of 10 to 16 per cryotube. Tissue was thawed and homogenized in 1 ml Trizol reagent (Gibco BRL/Life Technologies, Grand Island, NY) and glycogen, following the protocol provided by the manufacturer. Total RNA was stored at –80 °C in RNase-free water. Aliquots of total RNA in pooled samples are shown in Fig. 10.

Reverse transcription of total RNA—Integrity of total RNA was determined in an RNase-free 0.8% agarose gel. Quantity of total RNA was established using a spectrophotometer (BioRad Laboratories, Hercules, CA). Reverse transcription was accomplished with the Omniscript or Sensiscript kit (Qiagen, Valencia, CA), following the

protocol provided by the manufacturer and using approximately 2 μg (Omniscript) or 50 ng (Sensiscript) total RNA as template and oligo-dT or random hexamers as primer.

Table 2
Primer sequences used in PCR experiments

Primer pair	Primer sequence (5'→3')	Specificity	Product size
USalF mp1R	TTT GTC GAC GCT CTG TGC AGA CAT CTC TTC T GAT GTG GCG AGA TGC TCT TG	Transgene	3.9 kb
GAPDH-f GAPDH-r	TGA TGA CAT CAA GAA GGT GGT GAA G TCC TTG GAG GCC ATG TAG GCC AT	GAPDH	240 bp
LacZ3F mp1R	TTC AAC ATC AGC CGC TAC AGT C GAT GTG GCG AGA TGC TCT TG	Transgene	480 bp
USalF M13R	TTT GTC GAC GCT CTG TGC AGA CAT CTC TTC T GTT TTC CCA GTC ACG ACG TTG TAA	Transgene	376 bp
CRXneo-f CRXneo-r	ATG GAT TGC ACG CAG GTT CTC CTG ATG CTC TTC GTC CAG ATC	Mouse	285 bp
mCRX-f mCRX-r	GCA GCG ACA GCA GCA GAA ACA AGA AGC CGG GGC ATA GGT CAT	Mouse	310 bp
W149 W150	CAT CCC ACC TGA GCT CAC AGA AAG GCC TAC AAC AGA GGA GCT TCT AGC	Mouse *Pde6b*	298 bp
USalF UXbaR	TTT GTC GAC GCT CTG TGC AGA CAT CTC TTC T AAA TCT AGA ACC TCC TCT GCT GTC ACC T	Transgene	322 bp
HAU6-R HARE-3	GTG CTG GGA TTA CAG GCG TGA G CTG TAA ATT CTC CTG AAA GTC CCG CAG GAG	Human PDE6A upstream	1279 bp

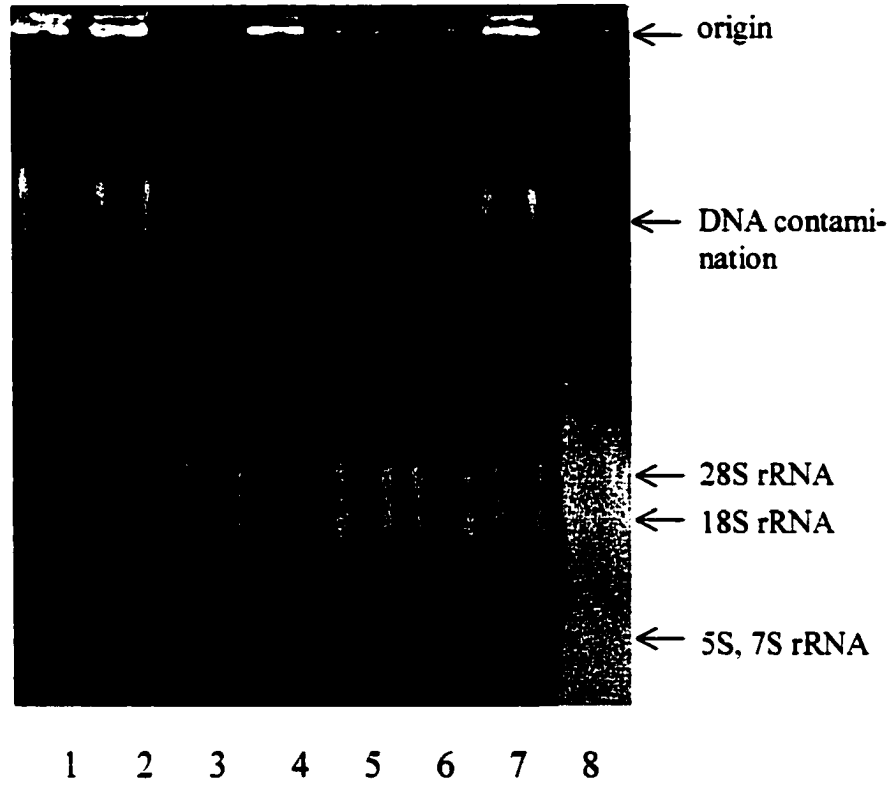

Fig. 10. *Crx*-/- 10- to 11-day-old mouse retina RNA samples used in RT-PCR. Total RNA was run on 0.8% RNase-free agarose mini-gel to assess integrity. *Lane number* corresponds to *Crx*-/- RNA sample number except for *lane 7*, which is a whole eye extract, and *lane 8*, which is the *rd*/+ 10-day-old positive control.

Amplification of cDNA—The cDNA was then amplified via PCR to determine presence of mRNA species, using specific primers shown in Table 3. For the primer pair mCRX-rt-f/mCRX-rt-r, the PCR reaction consisted of 0.5 µl reverse transcription product (cDNA) in a 25-µl reaction with 1 X PCR reaction buffer (Fisher buffer A: 50 mM KCl, 10 mM Tris-Cl pH 9.0, 0.1% Triton X-100, and 1.5 mM $MgCl_2$), 50 ng each primer, 0.2 mM dNTP mix, and 0.5 units Taq polymerase (Fisher Scientific, Pittsburgh, PA). PCR conditions were 5 min at 94 °C denaturation, followed by 35 cycles of 45 s at 94 °C denaturation, 45 s at 60 °C annealing, 45 s at 72 °C extension, and a final extension of 5 min at 72 °C. For primer pair mPDE6b-f/mPDE6b-r 6% DMSO was added to the above conditions. For primer pair mRHO1-f/mRHO1-r, the extension time was 120 s, with the same PCR conditions as above. For primer pairs mPDE6a-f/mPDE6a-r and W149/W150, the annealing temperature was 57 °C, with the same PCR conditions as above. PCR products were analyzed on 0.8% agarose gels (SeaKem, FMC Bioproducts, Rockland, ME).

Semi-quantitative RT-PCR—Total RNA samples used for reverse transcription were from *Crx-/-* 10- to 11-day-old mice and from 10-day-old *rd/+* and *rd/rd* mice as controls. Amplification of products by PCR was accomplished using the specific primer pairs mPDE6a-f/mPDE6a-r, mPDE6b-f/mPDE6b-r, mRHO2-f/mRHO2-r, mCRX-rt-f/mCRX-rt-r, and GAPDH-f/GAPDH-r in reactions as given above, but for 25 cycles of amplification (Table 3). PCR products were separated on 1X TBE 8% polyacrylamide gels at 100 V for approximately 20 min. Gels were stained in 1X TBE with ethidium bromide for 20 min, then destained in 1X TBE for 10 min. Stained gels were scanned

wet into the Typhoon 8600 Imaging system with medium sensitivity and 600 V photo-multiplier tube setting. Bands were identified, subjectively marked with rectangles, and analyzed with the spotfinder function in the Image Quant software program. The average volume of each band was compared with the average volume of the GAPDH band for the respective cDNA sample to obtain a GAPDH-normalized ratio. Each GAPDH-normalized ratio was compared to the average GAPDH-normalized ratio for the normal (*rd/+*), age-matched control. Experiments were repeated three times.

Table 3
Primer sequences used in RT-PCR experiments

Primer pair	Primer sequence (5'→3')	Specificity	Product size
GAPDH-f	TGA TGA CAT CAA GAA GGT GGT GAA G	GAPDH	240 bp
GAPDH-r	TCC TTG GAG GCC ATG TAG GCC AT		
mPDE6a-f	CCA TGC TGG ATG GGA TCA CTA AC	Mouse	241 bp
mPDE6a-r	CAG GGT GAC CTC CTC CTT CCT G		
mPDE6b-f	GTA TAC AAG GAA TTT TCT CG	Mouse	299 bp
mPDE6b-r	CAA ATT GCT ATA GGC AGA GTC CG		
mRHO1-f	GTG GTC CTG GCC ATT GAG CGC TAC G	Mouse	~1 kb
mRHO1-r	TCG TCA TCT CCC AGT GGA TTC TTG CC		
mRHO2-f	ATC CCT GAG GGC ATG CAA TGT TCA TG	Mouse	518 bp
mRHO2-r	CTG CTT GTT CAA CAT GAT GTA GAT GAC		
mCRX-rt-f	TGG AGG AGC TGG AGG CCC TGT TTG CCA A	Mouse	258 bp
mCRX-rt-r	CCA AAG GAT CTG TAC AAA CAT CTG TAG AG		
LacZ3F	TTC AAC ATC AGC CGC TAC AGT C	Transgene	480 bp
mp1R	GAT GTG GCG AGA TGC TCT TG		

Specific Aim 2

Generation of promoter plasmid constructs—The PDE6A promoter constructs used in Specific Aim 2 were previously generated in this lab (by Brandon White and Russ Taylor). The carrier plasmid used for all constructs is the promoterless pGL3 (Promega), in which the PDE6A promoter of interest was ligated to the firefly luciferase gene by using standard cloning techniques. The plasmid with no promoter or enhancer is designated pGL3-basic. A control plasmid for constitutive expression of luciferase is regulated by the cytomegalovirus (CMV) strong promoter and enhancer. Each promoter construct is derived from a 4.1-kb *Xba*I (New England Biolabs, Beverly, MA) /*Xho*I (Roche/Boehringer-Mannheim, Indianapolis, IN) restriction fragment of the upstream region of the PDE6A gene cloned into the plasmid pBluescript II KS (Stratagene, La-Jolla, CA). Primers complementary to the region of interest, USalF and UXbaR (Table 2), were designed to amplify a 322-bp segment upstream of the initiator methionine codon (ATG). This fragment was then cloned into the pBluescript II KS *Sma*I (New England Biolabs) restriction site to generate pBS-322 (see Fig. 5).

The pGL3-260 plasmid was generated by amplifying the pBS-322 plasmid with Pfu polymerase (Stratagene) using USalF and UXbaR primers, then digesting with *Stu*I (New England Biolabs). This 260-bp product was then purified and cloned into the *Sma*I site of pGL3-basic. The pGL3-300 plasmid was generated by digesting pBS-322 with *Sal*I (New England Biolabs) and *Nco*I (New England Biolabs) and then inserting the fragment into the *Xho*I/*Nco*I site of the pGL3-basic (promoterless) plasmid. The pGL3-1060 plasmid was generated by amplifying a 1279-bp fragment from pBS-4.1 with the primers HAU6-R and HARE-3 (Table 2), which are specific to this region. The PCR

product was purified and partially digested with *Nco*I (there are two *Nco*I sites within this fragment) to obtain the 1060-bp fragment. This 1060-bp fragment was cloned into the *Sma*I and *Nco*I sites of pGL3-basic. Plasmids containing mutated binding sites for CRX (TAA to CGG), pGL3-300-M13 and pGL3-300-M16, were generated using long oligonucleotides containing the DNA sequence change and then amplified by PCR using pBS-322 plasmid as template. The amplified product was digested with *Sal*I and *Nco*I and inserted into pGL3-basic at the *Xho*I/*Nco*I site. All plasmids were analyzed for correct size and orientation of the insert. The mutated plasmids were sequenced to verify mutations (Iowa State University Sequencing Facility, Des Moines, IA). The plasmids encoding pcDNA3.1-CRX-his (S. Chen), pMT3-NRL (A. Swaroop), and the NRL mutant pMT3-DD10 (A. Swaroop) were provided by collaborators.

Tissue culture of HEK 293 cells—The HEK 293 cell line consists of immortalized adherent human embryonic kidney cells. The cells were grown in flasks in Dulbecco's modified Eagle's medium (DMEM) (Gibco BRL/Life Technologies) with 5 or 10% fetal bovine serum (Hyclone, Logan, UT) and 1% penicillin/streptomycin/amphotericin B (Gibco BRL/Life Technologies) in 5% CO_2 at 37 °C. Cells were passaged at least once a week, depending on growth. To split confluent flasks, cells were first washed once or twice with 1X phosphate-buffered saline (PBS), then treated with 10 ml trypsin-EDTA (Gibco BRL/Life Technologies) for 5 min at room temperature to remove the adherent cells. Approximately 25 ml complete media (DMEM, 5% fetal bovine serum, 1% penicillin/streptomycin/amphotericin B) was added to inactivate the trypsin. The cells were centrifuged at 2000 rpm for 5 min to pellet. The media was removed, and cells

were resuspended in 10 ml complete media. To count cells, a 1:5 dilution was used on a Neubauer hemocytometer. At this point, cells were plated for transfection or reseeded in a clean flask with 35 ml complete media.

Transfections in HEK 293 cells—Transfections were carried out in 24-well plates, seeding approximately 8 X 10^4 cells per well to grow to 70-80% confluency overnight in 1 ml complete media. Transfections were accomplished using Polyfect reagent (Qiagen). The relative amounts of DNA used per well are given in Table 4. For transfections in triplicate, the amounts of DNA, serum-free DMEM, and Polyfect were tripled with a total volume of 350 µl and allowed to incubate at room temperature for 10 min. The mixtures were then diluted with 1 ml of complete media. Immediately before transfection, media on the cells was removed and replaced with 350 µl of complete media. The triplicate mixture was then added immediately to the cells, approximately 370 µl per well, and incubated for 4 h, at which time the media was removed and replaced with 1 ml of complete media. The transfected cells were incubated for approximately 48 h.

Luciferase assay of cell extracts—Cells were lysed in 100 µl of 1X passive lysis buffer (Promega), at room temperature for 5 min. Twenty microliters of cell lysate was added to a cuvette containing 100 µl Luciferase Assay System buffer II (Promega), according to the protocol, and light emission was measured immediately in a TD 20/20 luminometer (Turner Designs, Promega).

Table 4

Representative scheme for transfection in HEK 293 cells[a]

Reporter plasmid[b]	CRX[c]	NRL[c]	pcDNA3.1[d] (μg)
pGL3-basic	-	-	0.55
pGL3-260	-	-	0.55
pGL3-260	+	-	0.35
pGL3-260	++	-	0.15
pGL3-260	-	+	0.35
pGL3-260	-	++	0.15
pGL3-260	+	+	0.15
pGL3-260	++	++	0
pGL3-300	-	-	0.55
pGL3-300	+	-	0.35
pGL3-300	++	-	0.15
pGL3-300	-	+	0.35
pGL3-300	-	++	0.15
pGL3-300	+	+	0.15
pGL3-300	++	++	0
pGL3-1060	-	-	0.55
pGL3-1060	+	-	0.35
pGL3-1060	++	-	0.15
pGL3-1060	-	+	0.35
pGL3-1060	-	++	0.15
pGL3-1060	+	+	0.15
pGL3-1060	++	++	0
pGL3-control	-	-	0.55

[a]Each reaction was diluted with 165 μl serum-free DMEM.

[b]Approximately 0.4 μg reporter plasmid and 0.05 μg pRL-CMV (Renilla luciferase) were added to each reaction.

[c]The (-) symbol represents no plasmid added, the (+) symbol represents 0.2 μg added, and the (++) symbol represents 0.4 μg added to the reaction.

[d]pcDNA3.1 represents carrier plasmid DNA used to equalize the amount of plasmid used to 1 μg for all reactions.

Renilla luciferase assay—One hundred microliters Stop-n-Glo assay buffer (Promega) was added to the same cuvette in which the luciferase assay was performed. Light emission was measured immediately in the TD 20/20 luminometer.

Analysis of transfection assay results—The value obtained for each well in the luciferase (experimental) assay was divided by the value in the β-galactosidase or Renilla luciferase (internal controls) assay for the same well. This relative luciferase value was then compared with the relative luciferase value for each reporter plasmid alone in each experiment and recorded as fold stimulation compared with reporter plasmid alone. Averages of triplicate fold stimulation values were used to compare data within an experiment.

Oligonucleotide preparation for EMSA—Oligonucleotides were generated as shown in Table 5 (Gibco BRL/Life Technologies). Double-stranded oligonucleotides were generated by annealing single-stranded complementary oligonucleotides in a 1:1 molar ratio in 10 μl of 1X TEN buffer (0.3 M NaCl; 0.01 M Tris-HCl, pH 8; 0.001 M EDTA, pH 8) heated to 70 °C for 10 min and slowly cooled to room temperature (about 2 h). Oligonucleotides were labeled with α-^{32}P-dCTP with T4 polynucleotide kinase (MBI Fermentas) in a 10-μl reaction [1 X polynucleotide kinase buffer, 0.5 μl double-stranded oligonucleotide (approximately 25 ng), 1 μl T4 polynucleotide kinase, 0.5 μl α-^{32}P-dATP] that was heated at 37 °C for 30 min then at 90 °C for 2 min.

Protein preparation for EMSA—Bovine NRL protein was provided by Dr. Anand Swaroop (University of Michigan). Bovine CRX protein was synthesized using pcDNA3.1-CRX-His plasmid, provided by Dr. Shiming Chen (Washington University,

Table 5.
Sequences of oligonucleotides used in EMSA

Oligo	Sequence (5'→3')[a]	Protein[b]
CBE	ATG ACT TAA TCT CCC AAG CTT	CRX
TATA	CTT GAG AAA TAT TAA TGA CTT A	CRX
NRE	GAA CAC ACT GAT CCT CAT AAT CCT TGT TC	NRL
CBE/TATA	CTT GAG AAA TAT TAA TGA CTT AAT CTC CCA AGC TT	CRX
CBE/M13	CTT GAG AAA TAT TCC GGA CTT AAT CTC CCA AGC TT	CRX
M16/TATA	CTT GAG AAA TAT TAA TGA CTC CGT CTC CCA AGC TT	CRX
M16/M13	CTT GAG AAA TAT TCC GGA CTC CGT CTC CCA AGC TT	CRX
CBE/TATA/NRE	GAA CAC ACT GAT CCT CAT AAT CCT TGT TCT TGA GAA ATA TTA ATG ACT TAA TCT CCC AAG CTT	CRX/ NRL
CBE/TATA/AP1	GAA CAC ACT GAG TCA TAA TCC TTG TTC TTG AGA AAT ATT AAT GAC TTA ATC TCC CAA GCT T	CRX/ NRL

[a]All oligonucleotides are double-stranded, and the sense strand is shown.
[b]Proposed factor that binds to the oligonucleotide given.

St. Louis), as follows. HEK 293 cells were transfected with the pcDNA3.1-CRX-His plasmid using the lipofectin reagent method (Gibco BRL/Life Technologies), according to the protocol but scaled to a 60-mm culture dish. To do this, 500,000 HEK 293 cells were plated per 60-mm dish in four dishes and allowed to attach overnight. Ten micrograms of pcDNA3.1-CRX-His plasmid was added to 1 ml of serum-free DMEM, and 20 µl of lipofectin reagent was added to 1 ml serum-free DMEM in a separate mixture. After 30 min incubation at room temperature, these two solutions were combined and incubated for 10-15 min at room temperature, then added to 4.5 ml complete media in each of four dishes. Cells were incubated 16 h at 37 °C in 5% CO_2. Media was removed,

cells were washed twice in 1X PBS, and media was replaced with DMEM containing 5% fetal bovine serum. The cells were incubated 48 h at 37 °C in 5% CO_2 then lysed with 500 µl of 1X lysis buffer (Tropix) and centrifuged to pellet cell debris. CRX-His protein was partially purified in a 1-ml volume using the Ni-NTA His protein purification kit (Novagen) according to the protocol for batch method. Protein was confirmed on SDS-PAGE analysis with Coomassie blue or silver staining (data not shown).

EMSA—A representative scheme for an experiment is shown in Table 6. Protein-binding reactions were prepared on ice and consisted of 1X Gel Shift Buffer (12.5 mM Hepes, pH 7.9; 1.25% Ficoll 400; 0.5 mM $MgCl_2$; 1 mM dithiothreitol; 0.075 mM EDTA; 5% glycerol), 5 µl (approximately 2-8 µg total protein) total cell lysis, 200 µg polynucleotide deoxy-inosine:deoxy-cytosine, and 2 X 10^5 counts per minute of labeled oligonucleotide in a 20-µl reaction. All reagents except for the labeled oligonucleotide were incubated on ice for 15 min. After addition of oligonucleotide, reactions were incubated at room temperature for 20 min. Loading dye (4% Ficoll 400, 3 mg/ml xylene cyanol) was added as samples were loaded. Samples were electrophoresed in through a pre-run 6% (29:1) polyacrylamide:bisacrylamide native gel in 0.5X TBE buffer at 180 V for approximately 3 h. Gels were dried in a vacuum gel dryer and left to cool overnight. Dry gels were exposed to phosphor capture screens for 1 to 2 h. Screens were scanned on the Typhoon 8600 Imaging system and analyzed using Image Quant software.

Table 6
Representative scheme for EMSA

Labeled oligo	Protein extract[a]	Cold oligo[b]
CBE	-	-
CBE	HEK	-
CBE	HEK + CRX	-
CBE	HEK + CRX	CBE
CBE	HEK + CRX	TATA
CBE	HEK + CRX	CBE/TATA
CBE	HEK + CRX	-
TATA	-	-
TATA	HEK	-
TATA	HEK + CRX	-
TATA	HEK + CRX	TATA
TATA	HEK + CRX	CBE
TATA	HEK + CRX	CBE/TATA
TATA	HEK + CRX	-
CBE/TATA	-	-
CBE/TATA	HEK	-
CBE/TATA	HEK + CRX	-
CBE/TATA	HEK + CRX	CBE/TATA
CBE/TATA	HEK + CRX	CBE
CBE/TATA	HEK + CRX	TATA
CBE/TATA	HEK + CRX	-

[a]Protein extract is comprised of total cell lysis in passive lysis buffer of HEK 293 cells untransfected (HEK) or transfected with bovine CRX (HEK + CRX).
[b]Each cold oligo is titrated against the labeled oligo in steps of 1.5X, 10X, 50X, and 100X the concentration of the labeled oligo.

Specific Aim 3

Transgene construct—The construct used in developing the transgenic lines was generated in the plasmid pnLacF (a gift from Jacques Peschon, Immunex, Seattle, WA), in which the reporter gene bacterial β-galactosidase is ligated to the mouse protamine gene, a small gene encoding an intron, with a polyadenylation signal and site within the second exon. The promoter regions of interest were amplified from genomic DNA with the primer pair USalF/UXbaR (Table 2) (product approximately 300 base pairs sur-

rounding the tsp). The pnLacF plasmid was linearized with the restriction enzyme *KpnI* (Promega). The PCR products were purified and separately inserted by blunt-end cloning into the pnLacF *KpnI* site. The clones were selected on X-galactose (Gold Bio Technologies, St. Louis, MO) agar plates and analyzed for correct orientation and size. A correct plasmid was amplified in *Eschericia coli* in a 100-ml luria broth overnight culture and purified using a maxi-prep kit (Qiagen). The plasmids containing the correct inserts were labeled pnLacF-300. The plasmids were digested with *KpnI* and *BglII* (New England Biolabs) to release the entire promoter/β-galactosidase/ mouse protamine region. The digest products were purified in an intermediate step using 3 M sodium chloride and 100% ethanol to precipitate the product for the next digest. The *KpnI* digest was accomplished with 20 μg plasmid DNA, 1X digest reaction buffer, and 10 units of enzyme for 2 h at 37 °C. The *BglII* digest was accomplished with the precipitated digest product of the *KpnI* digest, 1X digest reaction buffer, and 10 units of enzyme for 2 h at 37 °C. The final product was precipitated, reconstituted, and confirmed on a 0.8% agarose gel stained in ethidium bromide (data not shown). A comparative map of the transgenic construct is shown in Fig. 11.

Transgenic mice—The purified digested product was sent to the Transgenic Animal Facility at the University of Alabama at Birmingham (Carl Pinkert, Director), where the constructs were microinjected into C57/B6 X SJL hybrid embryos. The facility screened for founders by PCR using the primers specific for the promoter region, USalF/M13R (Table 2), and agarose gel analysis. Mice shown to be positive for the transgene were separated into lines with three founders. The mice were phenotyped for

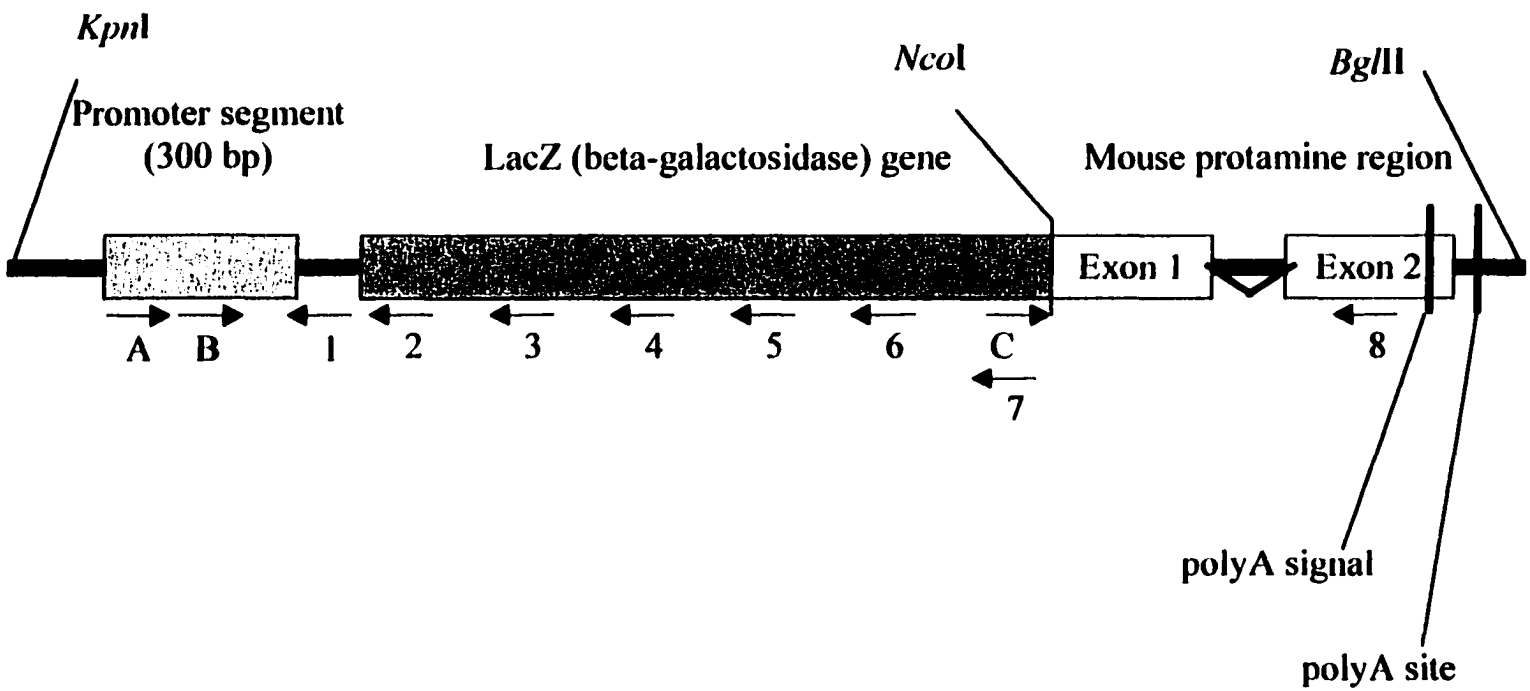

Fig. 11. Transgenic construct showing primer locations. Specific primers used in genotyping of transgenic mice are shown in relative location on the figure. Figure is not to scale. Forward primers: *A*, USalF; *B*, HARE4R; and *C*, LacZ3F. Reverse primers: *1*, M13R; *2*, LacZ-1; *3*, LacZ-2; *4*, LacZ-3; *5*, LacZ-4; *6*, LacZ-5; *7*, LacZ-6; and *8*, mp1R. Restriction sites for indicated restriction enzymes are given.

the *rd* allele of PDE6B, which causes retinal degeneration in the autosomal recessive state, as described below. The mice were bred to eliminate the *rd* allele. Mouse genetic and breeding information was documented using Cyrillic software (V 2.02, Cherwell Scientific Publishing, Palo Alto, CA) and Microsoft Access 2000 database software (V 9.0.2720, Microsoft, Seattle, WA). Mice were kept in a nonsterile room, with a 12-h light/dark cycle. Pups were weaned and separated by sex at 20-22 days and identified by ear punch. Tail samples (~1 cm) were also taken at this time. Mice were considered to be adult at 42 days and were usually mated at this time. Animals were usually sacrificed as adults (>60 days old), and tissues (retina, rest of eye, brain, lung, liver, kidney, and gonad) were removed and quick-frozen in either liquid nitrogen or a dry ice/ethanol bath. Care and use of these animals conformed to Institutional Animal Care and Usage Committee (IACUC number 000104662, Appendix).

Extraction of genomic DNA from tail samples—The tail samples were processed using the Wizard Genomic DNA Isolation kit (Promega), an inorganic method, according to the protocol. The tail samples were digested overnight in 1 ml nuclei lysis buffer with 35 μg/ml Proteinase K (Roche Laboratories, Indianapolis, IN) at 55 °C in a water bath. The samples were reconstituted in 1X TE buffer overnight and read by spectrophotometer (BioRad Laboratories). Aliquots of samples were diluted in water to 100 ng/μl for PCR amplification.

Genotyping of transgene—To confirm transmission of the transgene, each mouse was genotyped for the transgene promoter region by using the USalF and M13R PCR primers (Table 2) in a 25-µl reaction, using 100 ng of template genomic tail DNA, 1X PCR reaction buffer (Fisher buffer A: 50 mM KCl, 10 mM Tris-Cl pH 9.0, 0.1% Triton X-100, and 1.5 mM $MgCl_2$), 6% dimethyl sulfoxide, 50 ng each primer, 0.2 mM dNTP mix, and 0.5 units Taq polymerase (Fisher Scientific, Pittsburgh, PA). PCR conditions were 5 min at 94 °C denaturation, followed by 35 cycles of 45 s at 94 °C denaturation, 45 s at 55 °C annealing, 45 s at 72 °C extension, and a final extension of 5 min at 72 °C. A representative gel appears in Fig. 12.

Genotyping of rd allele—Genomic tail DNA was amplified by PCR using the primer pair W149/W150 (Table 2) in a 25-µl reaction using 100 ng of template DNA, 1X FailSafe PCR PreMix Selection Kit buffer D (Epicentre Technologies, Madison, WI), 50 ng of each primer, and 0.5 units of FailSafe PCR enzyme mix (Epicentre Technologies). PCR conditions were 5 min at 94 °C denaturation, followed by 35 cycles of 45 s at 94 °C denaturation, 45 s at 55 °C annealing, 45 s at 72 °C extension, and a final extension of 5 min at 72 °C. PCR products were confirmed on a 0.8% agarose gel. If the *rd* allele is present, the 298-bp PCR product will include extra restriction sites for the enzyme *Dde*I, yielding an upper band of 137 base pairs and lower bands of 105 and 45 base pairs. Therefore, the PCR products were then digested in a 10-µl reaction, consisting of 8 µl PCR product, 1X reaction buffer, and 8 units of *Dde*I enzyme (New England Biolabs).

The digest products were run on a 2% agarose gel to determine phenotype. Representative gels appear in Fig. 13.

Determination of the integrity of the transgene—To determine whether the transgene was intact in the mouse, a series of PCR amplifications were performed using reverse primers specific to different regions of the transgene with the same forward primer, HARE-4R (Table 2 and Fig. 11). The primers were primarily to the LacZ gene and are named LacZ-1 through 6 (Fig. 11). Another primer pair, LacZ3F/mp1R (Table 2), was used to amplify a product within the region joining LacZ with the mouse protamine gene. The primer pair USalF/mp1R amplifies the entire transgene from promoter to 3' end. All PCR reactions were performed in a 25- μl volume using 100 ng of template genomic tail DNA, 1X PCR reaction buffer (Fisher buffer A: 50 mM KCl, 10 mM Tris-Cl pH 9.0, 0.1% Triton X-100, and 1.5 mM $MgCl_2$), 6% dimethyl sulfoxide, 50 ng each primer, 0.2 mM dNTP mix, and 0.5 units Taq polymerase (Fisher Scientific). PCR conditions were 5 min at 94 °C denaturation, followed by 35 cycles of 45 s at 94 °C denaturation, 45 s at 55 °C annealing, 45 s at 72 °C extension, and a final extension of 5 min at 72 °C for the primer pair LacZ-1 (~500 base pairs); 90 s at 58 °C annealing and 120 s extension for primer pairs LacZ-2 (~840 base pairs), LacZ-3 (~1400 base pairs), and LacZ-4 (~2030 base pairs); and 90 s at 60 °C annealing and 180 s extension for primer pairs LacZ-5 (~2490base pairs) and *LacZ*-6 (~3000 base pairs). PCR conditions for primer pair LacZ3F/mp1R (~480 base pairs) were 5 min at 94 °C denaturation, followed by 35 cycles of 45 s at 94 °C denaturation, 45 s at 56 °C annealing, 45 s at 72°C extension, and a final extension of 5 min at 72 °C. PCR conditions for primer pair

Fig. 12. Representative genotyping of transgenic mice with primer pair USalF/M13R. Tail genomic DNA was amplified by PCR with the primers USalF and M13R. Presence of a band at approximately 400 base pairs indicates the presence of the transgene within the mouse. Likewise, absence of a band indicates absence of the transgene.

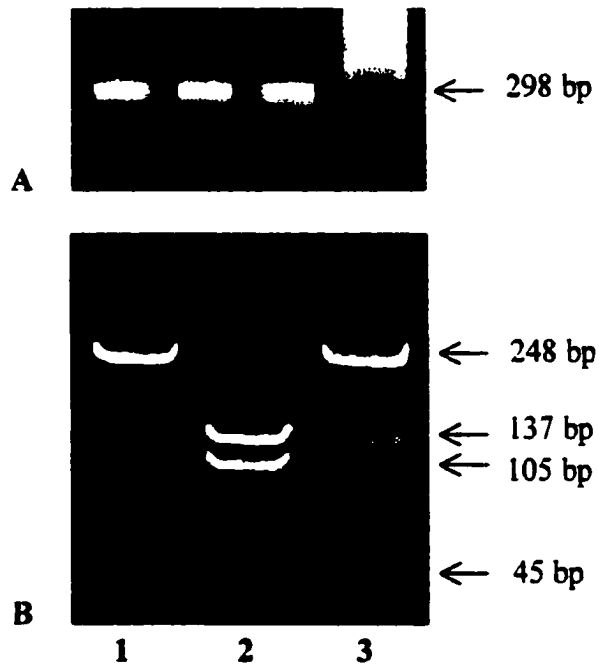

Fig. 13. Representative genotyping of *rd/rd* mice. Tail genomic DNA was first amplified by PCR to obtain a fragment of 298 base pairs (*A*). The *rd* allele contains two *Dde*I restriction sites. (*B*): Upon digestion with *Dde*I, three phenotypes can be seen that correspond with *rd* genotype: 248-bp band, wild-type (*lane 1*); 137-bp, 105-bp, and 45-bp bands, *rd/rd* (*lane 2*); 248-bp, 137-bp, 105-bp, and 45-bp bands, *rd/+* (*lane 3*).

USalF/mp1R (3.9 kilobase pairs) were 5 min at 94 °C denaturation, followed by 35 cycles of 1 min at 94 °C denaturation, 1 min at 60 °C annealing, and 3.5 min at 72 °C extension, and a final extension of 10 min at 72 °C.

β-galactosidase detection assay—Tissues were homogenized in 1X lysis buffer (Tropix). Tissue lysate was assayed using the Fluoreporter LacZ/galactosidase Quantitation Kit (Molecular Probes, Eugene, OR) according to the protocol. The assays were performed in a 96-well plate and read on a microplate reader (Fisher Scientific). A standard curve was generated using β-galactosidase enzyme (Promega).

Reverse transcriptase-PCR—Total RNA was extracted from tissues using Trizol reagent (Gibco BRL/Life Technologies) as per protocol in 1-ml samples, which included 1-6 retinas (1-3 mice) per sample or one piece of other tissue per sample. First-strand cDNA was generated using Omniscript or Sensiscript Reverse transcriptase kits (Qiagen) according to the protocol, using approximately 5 μg or 200 ng total RNA, respectively. Amplification of transcript was accomplished using primers specific to transgene mRNA, LacZ3F and mp1R (Table 3). Approximately 500 ng cDNA (0.5 μl of the reverse transcription reaction) was used in a 25 μl reaction with 1X PCR reaction buffer (Fisher buffer A: 50 mM KCl, 10 mM Tris-Cl pH 9.0, 0.1% Triton X-100, and 1.5 mM $MgCl_2$), 6% dimethyl sulfoxide, 50 ng each primer, 0.2 mM dNTP mix, and 0.5 units Taq polymerase (Fisher Scientific). PCR conditions were 5 min at 94 °C denaturation, followed

by 35 cycles of 45 s at 94 °C denaturation, 45 s at 56 °C annealing, 45 s at 72 °C extension, and a final extension of 5 min at 72 °C. Primers to endogenous GAPDH were used as a control (Table 3). The same PCR conditions as above were used, except the annealing temperature was 55 °C. PCR products were resolved on 0.8% agarose gels stained with ethidium bromide.

RESULTS

Specific Aim 1

Retinal cDNA of *Crx-/-* mice was amplified using PCR primers specific for cDNA for mouse *Pde6a*, *Pde6b*, *opsin*, and *Crx*. Results indicate that transcript of native PDE6A is present in the retinas of 10-day-old *Crx-/-* mice, as well as other transcripts from genes that also have CRX binding sites: PDE6B and rhodopsin. At 25 cycles of PCR, the product is in the linear range of amplification for the *Crx-/-* samples tested (Fig. 14, *upper photos*, 25X, *lanes 5-9*). Products became saturated between 25 and 35 cycles, at which it is apparent that transcripts are present in all samples for PDE6A, PDE6B, and rhodopsin (Fig. 14, *lower photos*, 35X, *lanes 5-9*). Products of amplification using *Crx*-specific primers were negative, as expected, in *Crx-/-* samples (Fig. 14*D*, *lanes 5-9*). Positive and negative controls gave expected results (Fig. 14, *lanes 1-4*): *rd/+* 10-day-old mice and normal adult mice were positive for all transcripts; *rd/rd* 10-day-old mice were positive for all transcripts, although, PDE6B was reduced at 25 cycles; and the negative control (no cDNA) was negative for each experiment.

Semi-quantitative analysis using imaging software and the Typhoon 8600 system demonstrated that transcript levels of the CRX influenced genes are altered, as shown in Table 7. PDE6A is indeed reduced in the *Crx-/-* mice approximately 40% compared to age-matched *rd/+* controls. Transcription of PDE6B was surprisingly increased in the knockout mice, with an increase of approximately 25% over control *rd/+* mice.

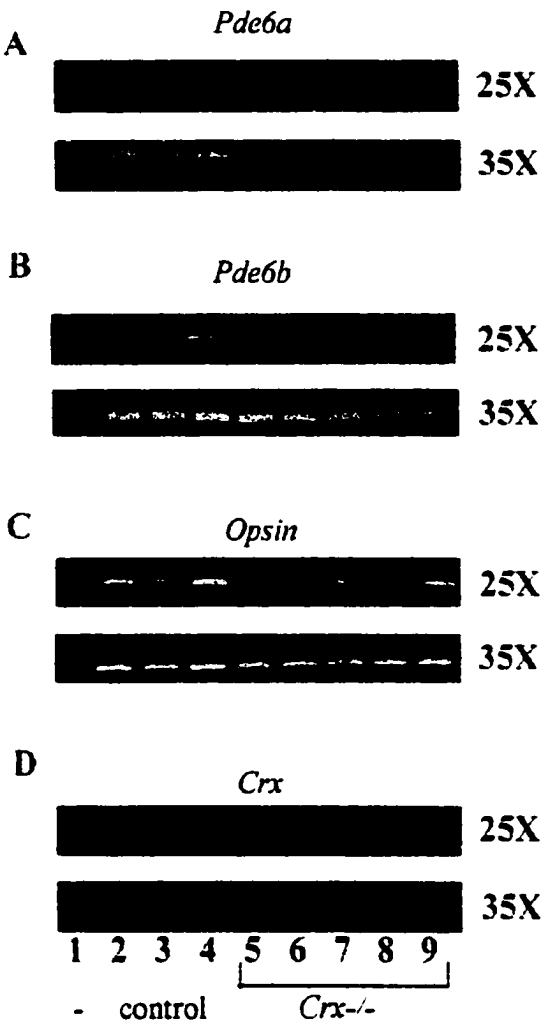

Fig. 14. Presence of specific transcripts in *Crx-/-* mice. Shown are RT-PCR products generated in 25 cycles (25X) or 35 cycles (35X) of PCR. A sizing ladder was run in a separate lane (not shown) to determine the approximate size of product. *Lane 1*, no cDNA negative control; *lane 2*, *rd/+* 10-day-old positive control; *lane 3*, *rd/rd* 10-day-old positive control; *lane 4*, normal adult >50-day-old positive control; *lane 5*, *Crx-/-* sample 3; *lane 6*, *Crx-/-* sample 4; *lane 7*, *Crx-/-* sample 5; *lane 8*, *Crx-/-* sample 6; *lane 9*, *Crx-/-* sample 7. All *Crx-/-* samples were from mice 10 to 11 days old, and each sample represents from 10 to 16 pooled mouse retinas.

Rhodopsin was shown to be decreased by approximately 50%. CRX transcript was non-detectable in all *Crx-/-* samples and was shown to be approximately 40% of GAPDH transcript level in control samples (Table 7).

Table 7.
Relative transcript levels in 10-day-old Crx-/- mouse retina as compared to 10-day-old control rd/+ mouse retina

Sample	*Pde6a*	*Pde6b*	*Crx*	*Opsin*
rd/+ 10-day-old	0.7033	0.3558	0.3644	1.7280
rd/rd 10-day-old	0.6520	0.3540	0.3493	1.5170
Normal adult	1.0241	0.3544	0.4786	1.5481
Crx-/- average[b]	0.4122	0.4682	nd[a]	0.8835
Percent control[c]	58.6%	131.6%	nd[a]	51.1%

[a]nd denotes not detected.
[b]*Crx-/-* average denotes the average GAPDH-corrected transcript level for all *Crx-/-* samples, N=8 with at least 2 trials of each sample.
[c]Average ratio denotes the ratio of the average *Crx-/-* sample GAPDH-corrected transcript level to the average normal GAPDH-corrected transcript level for the same gene.

Specific Aim 2

Using HEK 293 cells in culture, transfections were performed in which each of three constructs was transfected alone, with the transcription factor CRX, with the transcription factor NRL, or with both CRX and NRL. In performing experiments, however, an interesting phenomenon was seen in that the CRX and NRL plasmids appeared to have an effect on the internal control used. This phenomenon held true for both an SV40 promoter-driven β-galactosidase and for the CMV promoter-driven Renilla luciferase. The addition of CRX to an experiment resulted in a slight decrease in internal control activity, whereas the addition of NRL resulted in a highly increased internal

control activity. Experiments to confirm this phenomenon showed that there was indeed an increase in internal control activity when NRL was added to the internal control plasmid alone and a slight decrease, but not significant, when CRX was added alone. These results suggested that experimental values would be artificially high for CRX transactivation and artificially low for NRL transactivation. A mathematical adjustment was therefore devised to account for this difference while still making use of the internal control. These corrections were calculated and applied to experimental values to obtain a corrected relative luciferase fold stimulation value, which is reported as the following results.

The combined results of transfections involving pGL3-260, pGL3-300, and pGL3-1060 are shown in Figs. 15 and 16, in which at least five replications of each triplicate were performed, and each value is an average of at least 15 trials. The pGL3 plasmid with no promoter (pGL3-basic) and the pGL3 plasmid with a strong CMV promoter (pGL3-control) demonstrated consistent results in each experiment (data not shown). The basal transcription levels of each of the reporter plasmids, that is, without transcription factors present, approached zero. When plasmid encoding CRX or NRL was added, the expression of reporter increased, with varying levels that depended on the length of the construct and on the concentration of the transcription factor plasmid used. CRX and NRL added separately had about the same effect on the same construct, approximately 4-fold and 3-fold for smaller amounts (CRX or NRL) and 7-fold and 6-fold for larger amounts [2(CRX) or 2(NRL)] of transcription factor for pGL3-260 (Fig. 15). Fold stimulation values were 3-fold and 4-fold for smaller amounts and 9-fold and 8-fold for larger amounts of CRX and NRL for pGL3-300 (Fig. 15). Fold stimulation

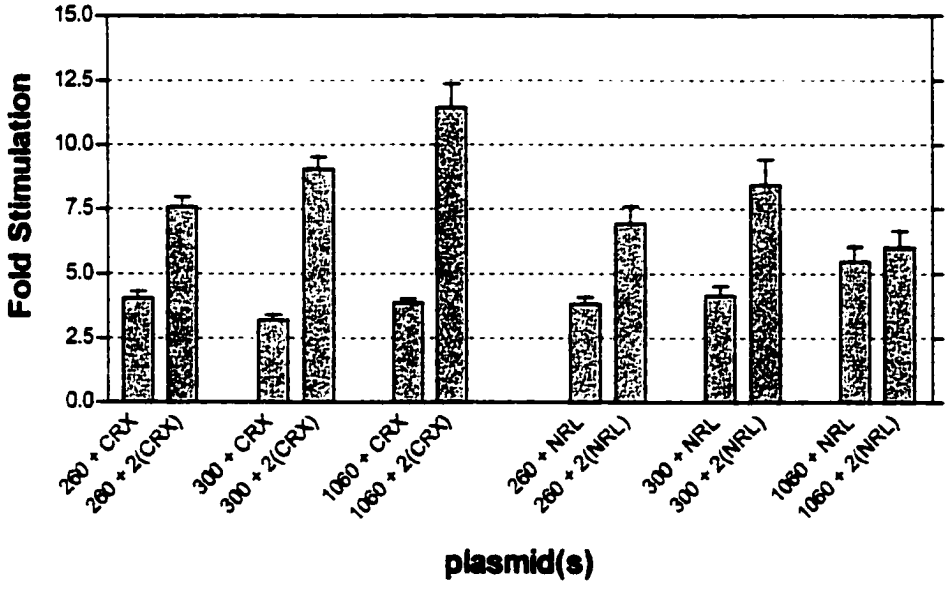

Figure 15. Effects of transcription factors CRX and NRL on PDE6A promoter fragments of 260-, 300-, and 1060-bp length in transient transfection experiments. *Error bars* denote the standard error of the mean. The number of replicates for each combination of plasmids was at least 15. Fold stimulation is expressed as the ratio of the experimental corrected relative luciferase value to the relative luciferase value for the respective reporter plasmid alone (e.g., 260 + CRX value divided by the 260 average value in the same triplicate). The amount of transcription factor used in CRX and NRL combinations was doubled for the 2(CRX) or 2(NRL) combinations.

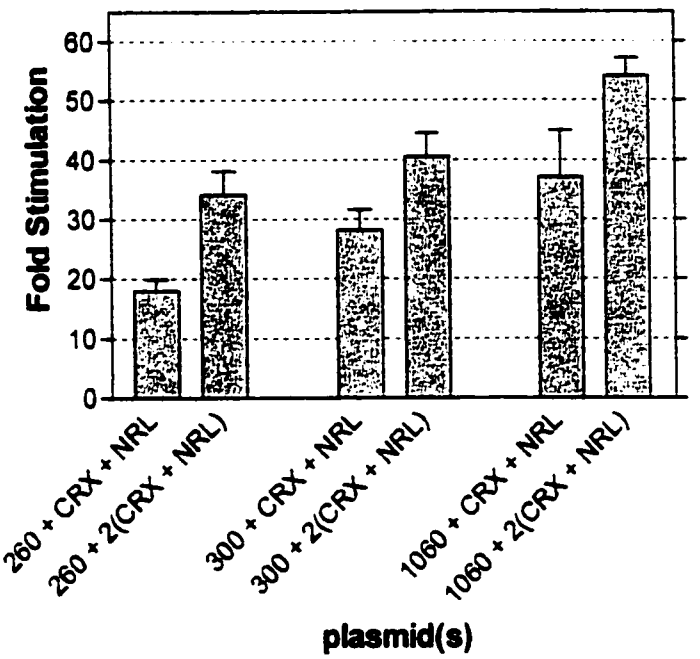

Figure 16. Effects of both transcription factors CRX and NRL together on PDE6A promoter fragments of 260-, 300-, and 1060-bp length in transient transfection experiments. *Error bars* denote the standard error of the mean. The number of replicates for each combination of plasmids was at least 15. Fold stimulation is expressed as the ratio of the experimental corrected relative luciferase value to the relative luciferase value for the respective reporter plasmid alone (e.g., 260 + CRX + NRL value divided by the 260 average value in the same triplicate). The amount of transcription factor used in CRX + NRL combinations was doubled for the 2(CRX + NRL) combinations.

values were 4-fold and 5-fold for smaller amounts and 11-fold and 6-fold for larger amounts for pGL3-1060 (Fig. 15). When CRX and NRL were cotransfected with one of the three reporter plasmids, a synergistic effect was seen for all three (Fig. 16). The degree of synergism was shown to be greater than the additive effect of CRX and NRL transactivation alone: approximately 2.3-fold (sum = 7.90) and 2.4-fold (sum = 14.5) greater for pGL3-260, 3.8-fold (sum = 7.37) and 2.3-fold (sum = 17.5) for pGL3-300, and 4-fold (sum = 9.36) and 3.1-fold (sum = 17.5) greater for pGL3-1060 for smaller and larger amounts of plasmid, respectively.

To test the assumption that CRX and NRL were binding to conserved sites within the proximal promoter that show a retina-specific footprint in previous experiments (that is, the CBE and TATA box region, Fig. 6), mutants were generated in which one of these sites was mutated so that the consensus CRX binding sequence was disrupted. The mutant M13 corresponds to the TATA site, and the mutant M16 corresponds to the CBE site, as shown in Fig. 7. In the absence of transcription factors, the expression of M13 and M16 constructs was essentially zero (data not shown). When CRX or NRL was added, expression increased and was approximately 1.2- to 1.4-fold the expression of the pGL3-300 construct for M13 but only 0.28- to 0.62-fold for M16 (Fig. 17). When both CRX and NRL were added, expression was approximately 2.3 times greater for M13 and 2.4 times less for M16 compared with pGL3-300 cotransfected with CRX and NRL (Fig. 18). Transactivation resulting from synergism of CRX and NRL was highest for the M13 reporter plasmid and was approximately 5.6-fold that of M16 (Fig. 18).

To demonstrate the difference in relative luciferase values that is caused by the internal control interaction phenomenon, average fold stimulation values are shown for

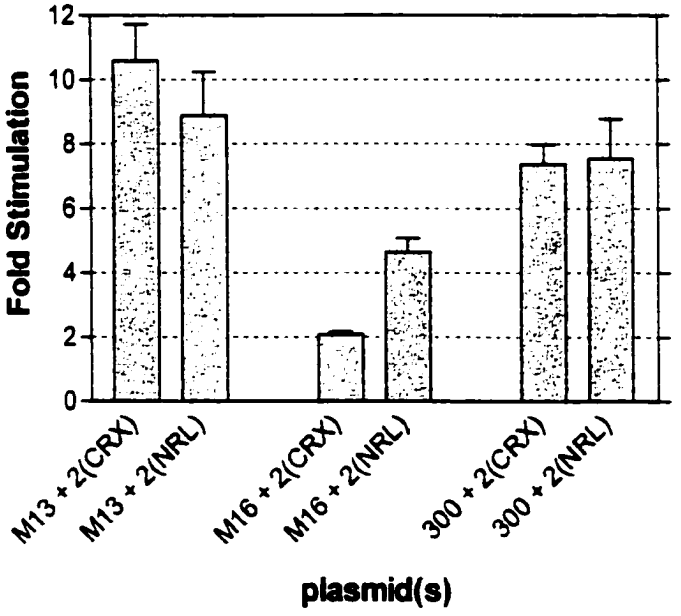

Figure 17. Effects of transcription factors CRX and NRL on PDE6A mutant promoter fragments M13 and M16 in transient transfection experiments as compared with the 300-bp PDE6A promoter fragment. *Error bars* denote the standard error of the mean. The number of replicates for each combination of plasmids was at least 21. Fold stimulation is expressed as the ratio of the experimental corrected relative luciferase value to the relative luciferase value for the respective reporter plasmid alone (e.g., M13 + 2(CRX) value divided by the M13 average value in the same triplicate). The amount of transcription factor used in CRX and NRL combinations (Figs. 15, 16) was doubled for the 2(CRX) or 2(NRL) combinations.

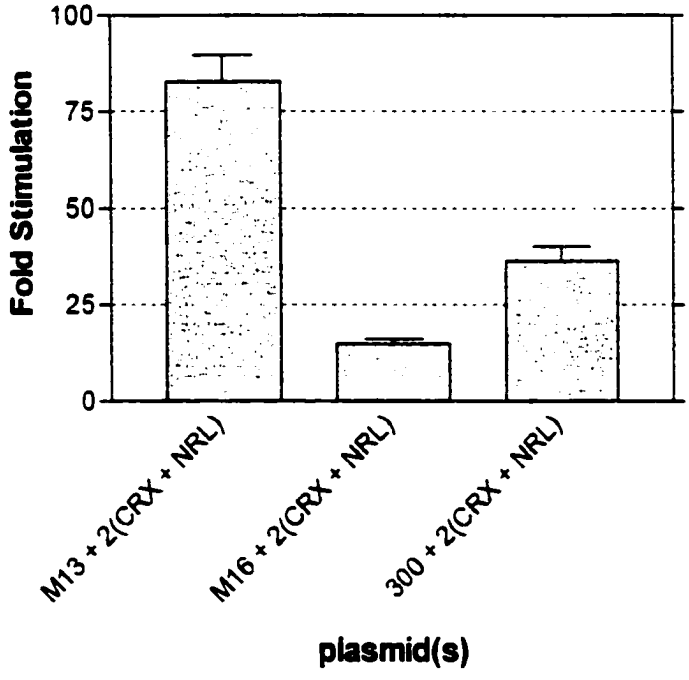

Figure 18. Effects of both transcription factors CRX and NRL together on PDE6A mutant promoter fragments M13 and M16 in transient transfection experiments compared with the 300-bp PDE6A promoter fragment. *Error bars* denote the standard error of the mean. The number of replicates for each combination of plasmids was 21. Fold stimulation is expressed as the ratio of the experimental corrected relative luciferase value to the relative luciferase value for the respective reporter plasmid alone (e.g., M13 + 2(CRX + NRL) value divided by the M13 average value in the same triplicate). The amount of transcription factor used in CRX + NRL combinations (Figs. 15, 16) was doubled for the 2(CRX + NRL) combinations.

pGL3-300 in Fig. 19 as a comparison of corrected and uncorrected values. The greatest effect can be seen in experiments that involved the addition of NRL with an approximate 4-fold difference between corrected and uncorrected values (Fig. 19). When plasmids are added together, the decrease due to internal control interaction is approximately 2.25-fold (Fig. 20).

EMSA results showed no effect of salt concentration on binding as demonstrated by band shift in the range of 0 to 100 mM magnesium chloride (data not shown). There was also no effect on binding when NRL was added to any of the oligonucleotides tested (see Fig. 23). Purified CRX protein demonstrated a single band at the upper position indicated in Figs. 22-24; however, imaging quality prevented distinguishable photo images of the gels. When the CRX homeodomain protein (that is, a protein containing only the short DNA-binding domain) was added to each oligonucleotide alone, a specific lower band was apparent for most oligonucleotides studied, although the intensity of the shifted band varied depending on the binding sites present (Fig. 21). The binding was apparently strongest in the CBE/TATA, CBE/TATA/ NRE, and CBE/TATA/AP1 oligonucleotides, as shown by dark bands, and was absent in the M13/M16 double-mutant oligonucleotide.

When a cell extract containing CRX was added, however, all oligonucleotides showed some shift in position relative to free oligonucleotide. As shown in Figs. 22-24, a specific shift occurred when cell extract containing expressed CRX (HEK/CRX) was added to the gel shift mixture, compared with a mixture containing cell extract without CRX expressed (HEK). This specific shift is competed away with unlabeled oligonucleotide, whether with self or with other CRX binding oligonucleotides (Figs. 22-24).

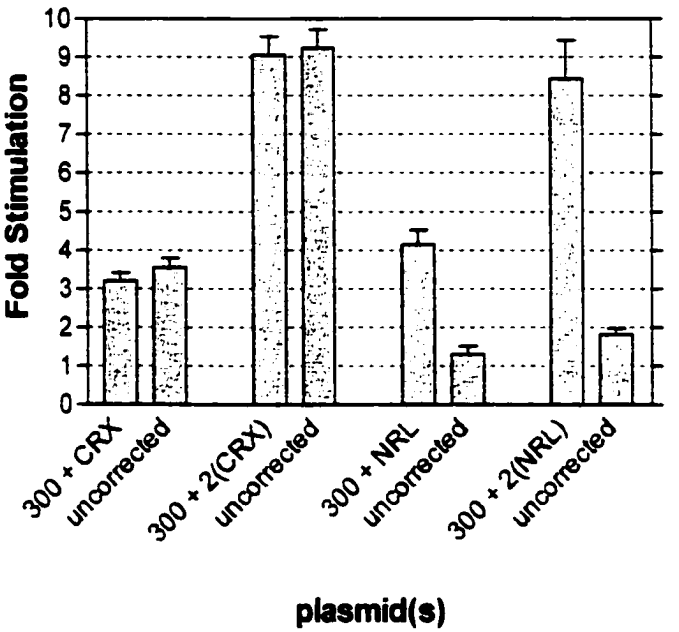

Fig. 19. Effect of mathematical correction on experimental fold stimulation values for CRX and NRL. *Error bars* denote the standard error of the mean. The corrected fold stimulation values are shown compared with respective uncorrected values for the reporter pGL3-300 only. The number of replicates for each combination of plasmids was 15.

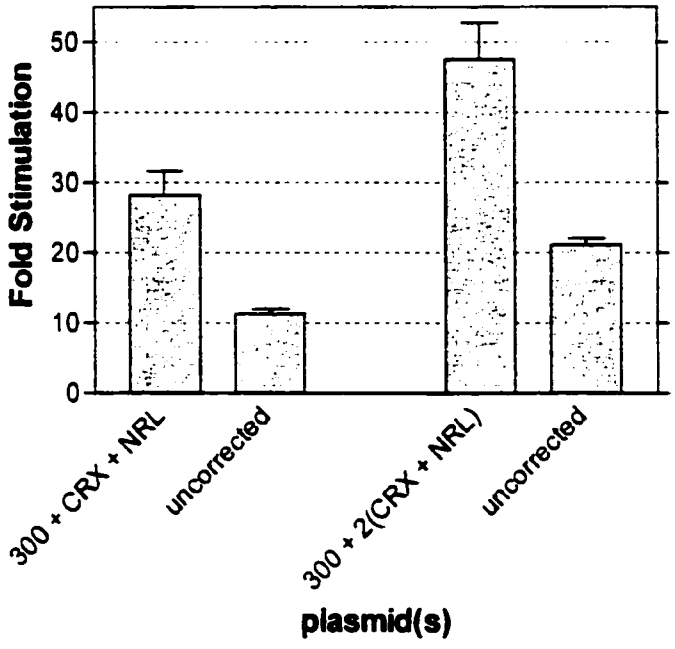

Fig. 20. Effect of mathematical correction on experimental fold stimulation values for CRX and NRL combined. *Error bars* denote the standard error of the mean. The corrected fold stimulation values are shown compared with respective uncorrected values for the reporter pGL3-300 only. The number of replicates for each combination of plasmids was 15.

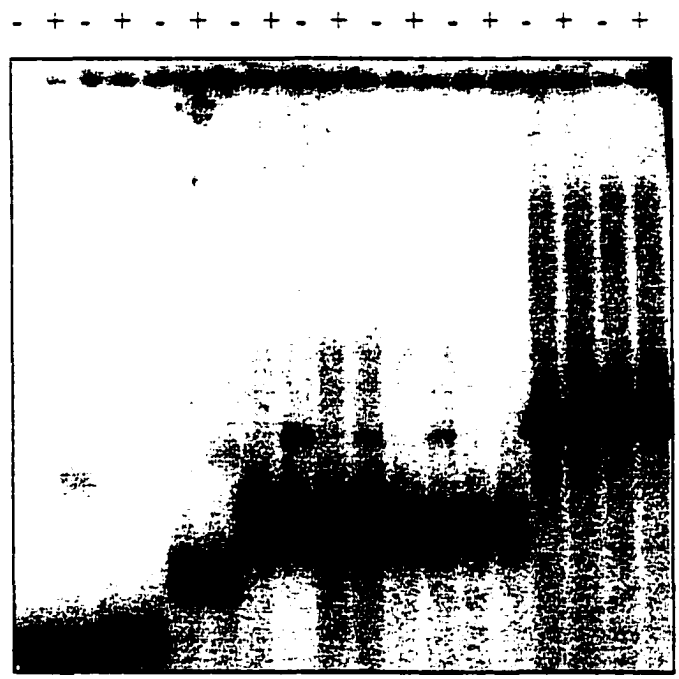

Fig. 21. EMSA of the truncated CRX homeodomain protein with labeled oligonucleotides. Oligonucleotide alone (-) or with CRX homeodomain protein added (+) was assayed for binding.

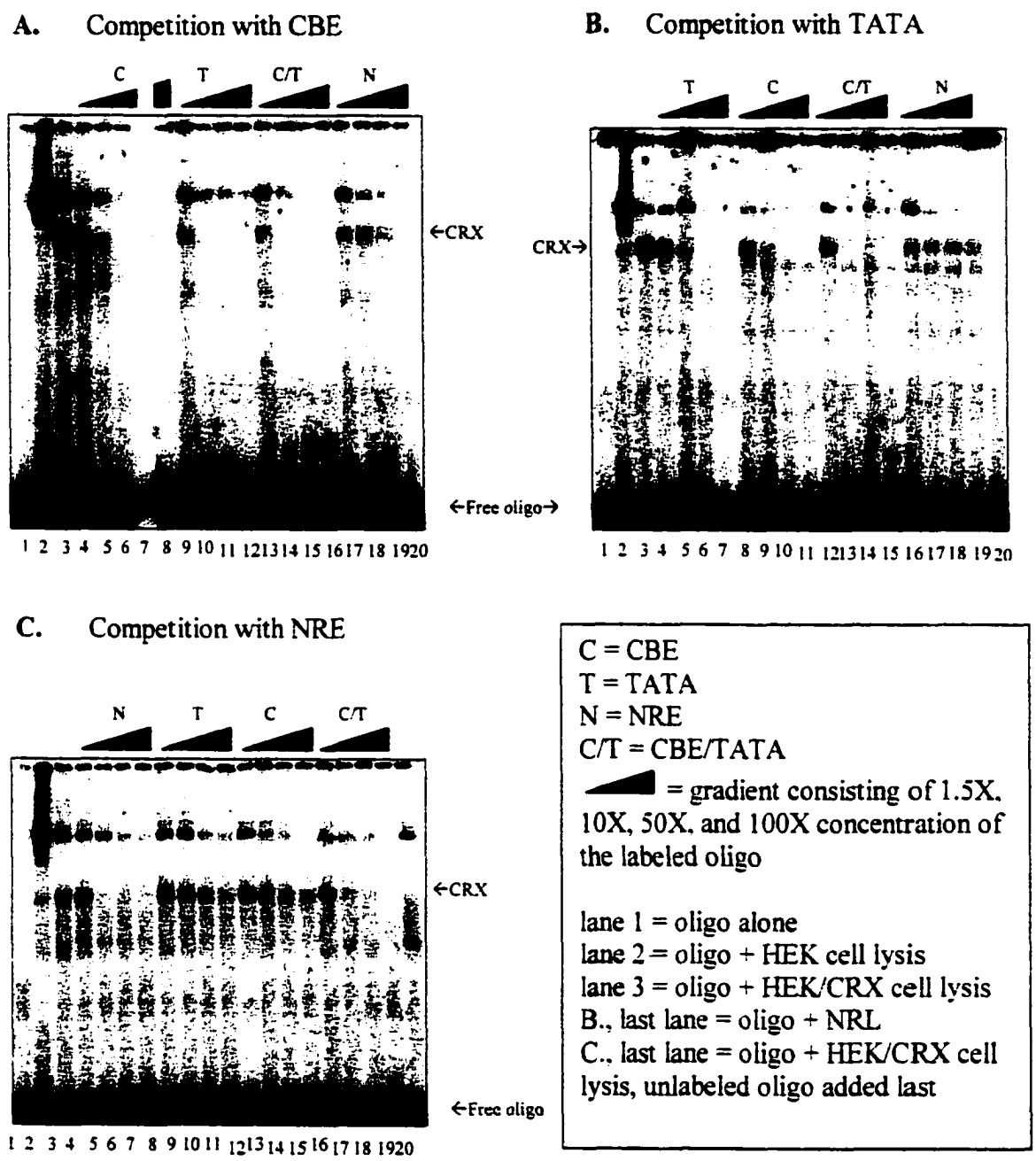

Figure 22. Competition with unlabeled oligonucleotides against short, labeled oligonucleotides. Results of electrophoretic mobility shift assay in which the CBE, TATA, and NRE labeled oligonucleotides are competed from CRX with unlabeled oligonucleotides as shown in the figure and legend.

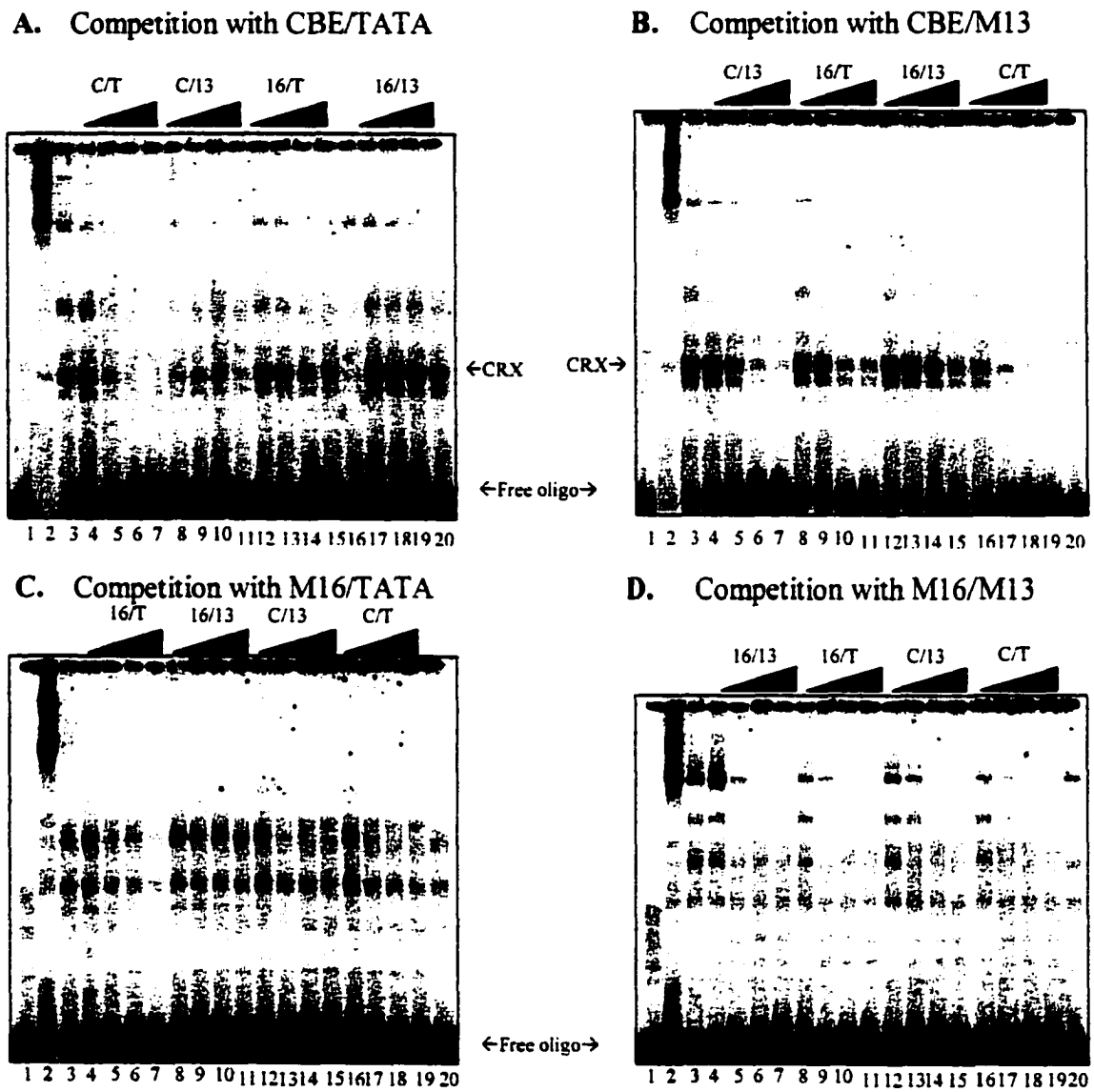

C/T = CBE/TATA
C/13 = CBE/M13
16/T = M16/TATA
16/13 = M16/M13
▲ = gradient consisting of 1.5X, 10X, 50X, and 100X concentration of the labeled oligo

lane 1 = oligo alone
lane 2 = oligo + HEK cell lysis
lane 3 = oligo + HEK/CRX cell lysis
A., lane 16 = oligo + HEK/CRX cell lysis, unlabeled oligo added last
B., C., and D. last lane = oligo + HEK/CRX cell lysis, unlabeled oligo added last

Figure 23. Competition with unlabeled oligonucleotides against medium-sized, labeled oligonucleotides. Results of electrophoretic mobility shift assay in which the CBE/TATA, M16/TATA, CBE/M13, and M16/M13 labeled oligonucleotides are competed from CRX with unlabeled oligonucleotides as shown in the figure and legend.

A. Competition with CBE/TATA/NRE

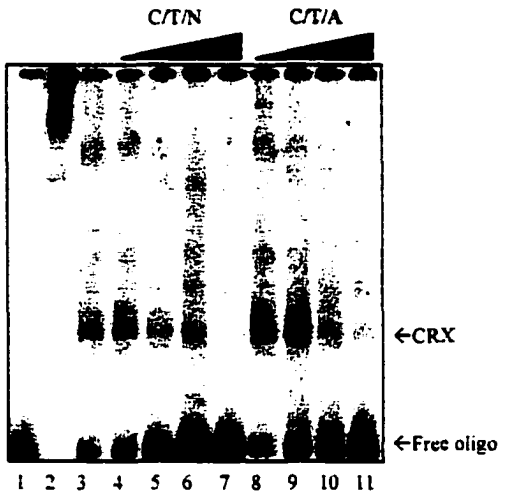

B. Binding of NRL to CBE/TATA/NRE

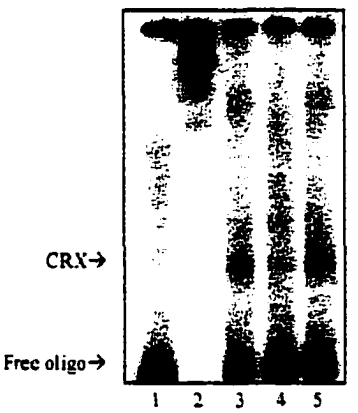

C. Competition with CBE/TATA/AP1

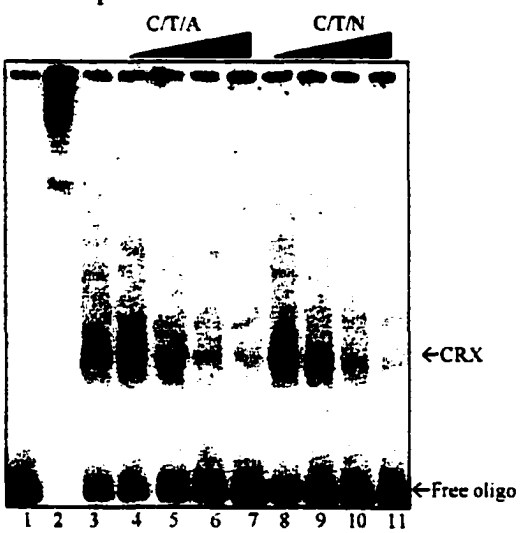

D. Binding of NRL to CBE/TATA/AP1

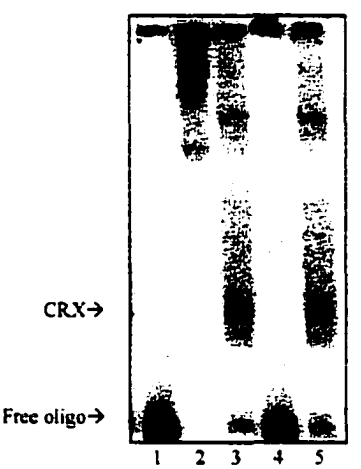

C/T/N = CBE/TATA/NRE
C/T/A = CBE/TATA/AP1
◢ = gradient consisting of 1.5X, 10X, 50X, and 100X concentration of the labeled oligo

lane 1 = oligo alone
lane 2 = oligo + HEK cell lysis
lane 3 = oligo + HEK/CRX cell lysis
lane 4 = oligo + NRL
lane 5 = oligo + HEK/CRX cell lysis +NRL

Figure 24. NRL binding to and competition with unlabeled oligonucleotides against long, labeled oligonucleotides. Results of electrophoretic mobility shift assay in which the CBE/TATA/NRE and CBE/TATA/AP1 labeled oligonucleotides are competed from CRX with unlabeled oligonucleotides and mixed with NRL as shown in the figure and legend.

EMSA with the short oligonucleotides (that is, CBE, TATA, and NRE) are shown in Fig. 22. In *lane 1* of each gel the free oligonucleotide is apparent at the bottom of the photograph. Shifted bands in *lane 2* of each gel are due to intrinsic factors in the HEK 293 cells used. In the presence of expressed CRX (*lane 3*) a single band is shifted for the oligonucleotides CBE, TATA, and NRE (Fig. 21*A*, *B*, *C*, *lane 3*). Results from competition assays demonstrate that unlabeled oligonucleotide competes for binding to CRX with labeled oligonucleotide (Fig. 22). It is apparent that labeled CBE is competed from CRX by unlabeled self (Fig. 22*A*, *lanes 4-6, 8*), as well as TATA (Fig. 22*A*, *lanes 9-12*), CBE/TATA (Fig. 22*A*, *lanes 13-16*), and NRE weakly (Fig. 22*A*, *lanes 17-20*). Competition against labeled TATA demonstrated that TATA (Fig. 22*B*, *lanes 4-7*), CBE (Fig. 22*B*, *lanes 8-11*), and CBE/TATA (Fig. 22*B*, *lanes 12-15*) were able to compete away CRX, whereas NRE (Fig. 22*B*, *lanes 16-19*) could not compete. Competition with labeled NRE demonstrated that each unlabeled oligonucleotide was able to compete for CRX: NRE (Fig. 22*C*, *lanes 4-7*) strongly, TATA weakly (Fig. 22*C*, *lanes 8-11*); CBE weakly (Fig. 22*C*, *lanes 12-15*) and CBE/TATA strongly (Fig. 22*C*, *lanes 16-19*).

Medium-length oligonucleotides that are comprised of two sites are represented in Fig. 23. The CBE/TATA oligonucleotide displays a lower gel-shifted band when CRX is added (Fig. 23*A*, *lane 3*) compared with HEK lysis alone (Fig. 23*A*, *lane 2*) or free oligonucleotide (Fig. 23*A*, *lane 1*). The two mutant sites M13 and M16 were present on longer oligonucleotides comprised of two sites in three combinations (CBE/M13, M16/TATA, and M16/M13) and were able to bind protein demonstrated by band shifts (Fig. 23*B*, *C*, and *D*, *lane 3*) when compared with HEK lysis alone (Fig. 23*B*, *C*, and *D*, *lane 2*) or free oligonucleotide (Fig. 23*B*, *C*, and *D*, *lane 1*). It is apparent in Fig. 23 that

the specific bands attributed to CRX binding in photos *A* and *B* are not present in photos *C* and *D*. In competition studies, unlabeled CBE/TATA was able to strongly compete CRX from CBE/TATA and CBE/M13 oligonucleotides (Fig. 23*A*, *lanes 4-7*; *B*, *lanes 16-19*). Unlabeled CBE/TATA (Fig. 23*A*, *lanes 4-7*) was able to strongly compete and CBE/M13 (Fig. 23*A*, *lanes 8-11*) was able to weakly compete for binding with CBE/TATA, whereas M16/TATA and M16/M13 were unable to compete (Fig. 23*A*, *lanes 12-15*, *17-20*). The band shifts caused by labeled CBE/M13 were competed away by self (Fig. 23*B*, *lanes 4-7*), by M16/TATA weakly (Fig. 23*B*, *lanes 8-11*), and by CBE/TATA very strongly (Fig. 23*B*, *lanes 16-19*), but were not competed by M16/M13 (Fig. 23*B*, *lanes 12-15*). Shifted bands were not present with M16/TATA and, therefore, competition was obvious only for non-specific binding of intrinsic HEK factors.

Oligonucleotides containing all three sites within the CRX footprinted region also demonstrated band shifts upon addition of expressed CRX (Fig. 24, *lane 3*). The mutated NRE-like site (AP1) appeared to have no effect on binding, and a supershift was not seen when CRX and NRL were added together to either CBE/TATA/NRL or CBE/TATA/AP1 oligonucleotides (Fig. 24*B*, *D*, *lane 5*). Competition experiments demonstrated that unlabeled CBE/TATA/NRE was able to compete against labeled self (Fig. 24*A*, *lanes 4-7*) and unlabeled CBE/TATA/AP1 (Fig. 24*C*, *lanes 8-11*). Unlabeled CBE/TATA/AP1 is able to compete for CRX binding with labeled CBE/TATA/NRL (Fig. 24*A*, *lanes 8-11*) as well as labeled self (Fig. 24*C*, *lanes 4-7*). Interestingly, the shorter oligonucleotide CBE/TATA strongly competed away labeled CBE/TATA/NRE and CBE/TATA/AP1 (data not shown).

Specific Aim 3

The study under Specific Aim 3 involved the establishment of a mouse colony in which a short fragment of approximately 300 base pairs surrounding the major transcription start point in the PDE6A promoter was ligated to the bacterial β-galactosidase reporter gene to determine the minimum photoreceptor-specific promoter necessary for proper spatial expression of the reporter gene. Three lines were identified in the colony, and each mouse was genotyped via PCR for a segment of the transgene using the specific primers USalF and M13R (Table 2), which amplified a product 376 base pairs in length. Mice positive for the transgene and negative for the *rd/rd* genotype were bred, then sacrificed and dissected to collect retina, rest of eye, brain, lung, heart, liver, kidney, and gonad tissues. Data presented in this section were previously published (71).

None of the mice assayed were able to demonstrate any measurable β-galactosidase activity, either in solution assay or in histochemical section analysis. Because of the confounding results, we performed RT-PCR on retina and tissue samples. PCR using cDNA-specific primer pair LacZ3F/mp1R (Table 3) to the β-galactosidase portion of the transgene amplified a 480-bp product of the transgene transcript in retina as well as brain, but not in other tissues (Fig. 25). Transcript level in brain varied among the three lines: very strong in line 7-2, very weak in line 9-5, and weak in line 9-11 (Fig. 25, *lane B*). Multiplex PCR demonstrated that all samples were positive for the endogenous GAPDH gene PCR product as determined by the presence of a 240-bp specific product (Fig. 25).

In situ hybridization of retina and brain localized the transgene transcript to the outer retina, more specifically the rod inner segments (RIS) (Fig. 26*A*), and to portions of the cerebellum (data not shown). Probes used in the *in situ* studies were specific for the

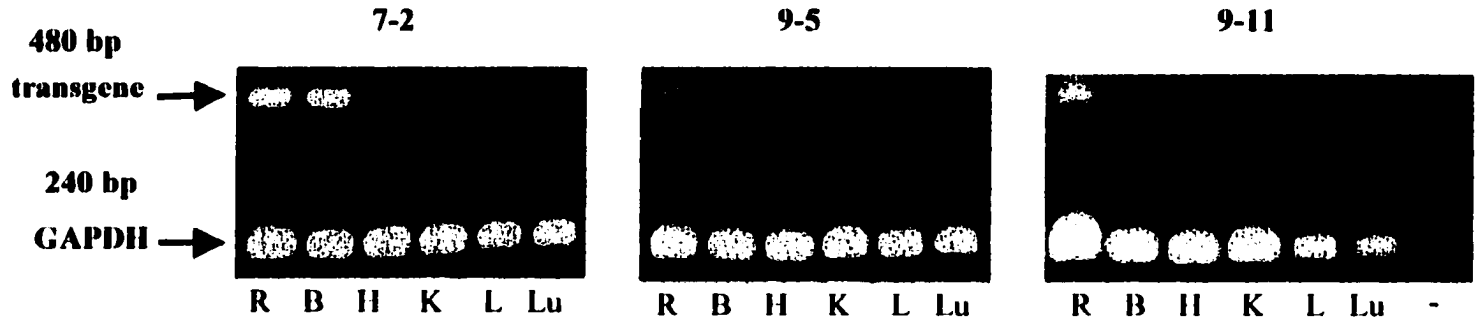

Fig. 25. Presence of transcript in transgene-positive mouse retina. Results of multiplex RT-PCR in which transgene-specific primer pair USalF/M13R was used to determine the presence of transgene mRNA in tissue samples. Primers complementary to the endogenous glyceraldehyde-3-phosphate dehydrogenase (GAPDH) were used as a control. Transgene-specific bands were seen in retina in all three lines. A transgene-specific band was also seen in brain for all three lines, although at varying levels: 7-2, strong; 9-5, very weak; 9-11, weak. Each gel represents one mouse in each line. R, retina; B, brain; H, heart; K, kidney; L, liver; Lu, lung; -, no template added. Adapted from Taylor et al., 2001 (71).

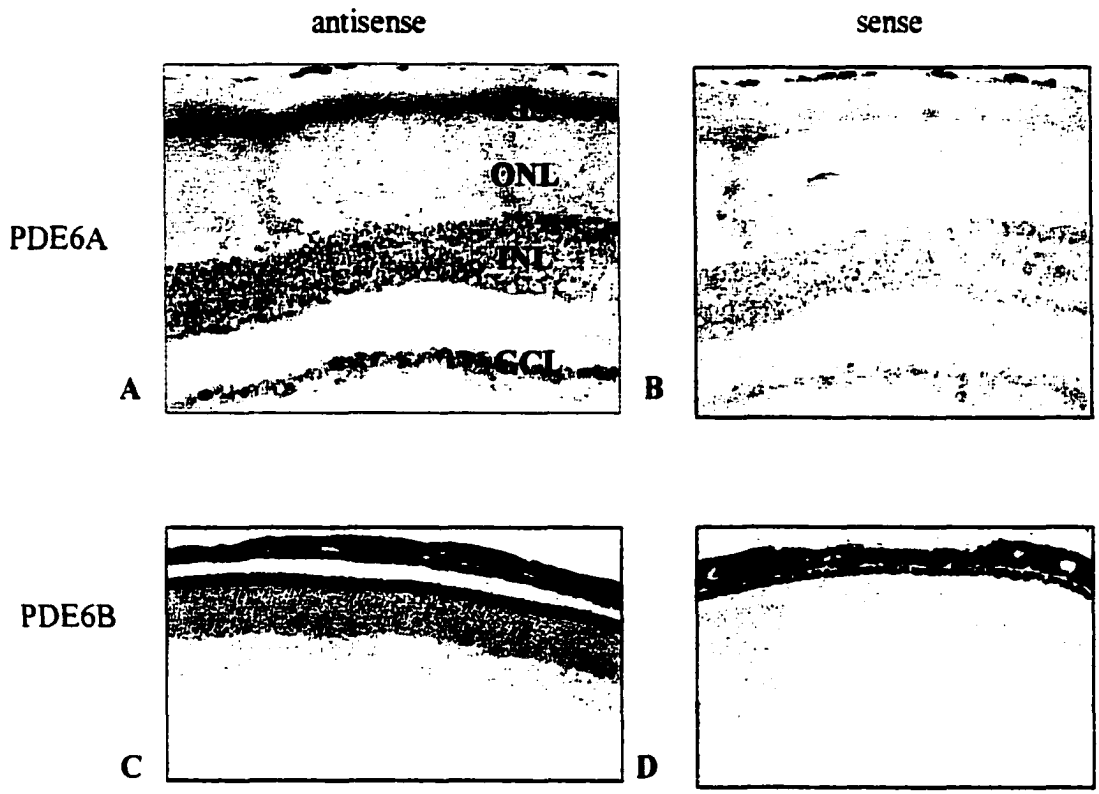

Fig. 26. *In situ* hybridization analysis of transgene-specific transcript in transgene-positive mouse retina. Slides shown are representative of mice in line 7-2. Probes were digoxigenin-labeled transgene-specific PCR products generated through RT-PCR. Probes to PDE6B were used as a retina-specific control. Antisense probe to PDE6A transgene is located primarily in the inner segments (RIS) of the photoreceptor layer. Sense probe was negative as expected. Antisense probe to PDE6B is located primarily in the RIS as well, and sense probe was negative. Probe to transgene was also localized to cerebellum (data not shown). RIS, rod inner segment; ONL, outer nuclear layer; INL, inner nuclear layer; GCL, ganglion cell layer. Adapted from Taylor et al., 2001 (71).

β-galactosidase portion of the transgene (experimental) and endogenous PDE6B, a marker for photoreceptor-specific transcription (control). In Fig. 26*A*, a representative slide of mice in line 7-2 is shown in which the antisense probe localizes the mRNA of the transgene to the photoreceptor layer, or rod inner segment (RIS) layer, but the sense probe in Fig. 26*B* does not produce an equal effect. The image in Fig. 26*C* shows the antisense probe localizing PDE6B transcript to the outer nuclear layer (especially RIS), as would be expected; however, it would be expected that no staining would occur in Fig. 26*D* using a sense probe.

DISCUSSION

Specific Aim 1

The expression of PDE6A in CRX knockout mice implies that CRX is not absolutely required for PDE6A expression. In addition, the expression of other genes that also contain CRX binding sites within their promoters implies that CRX is not required for low-level expression of rhodopsin or PDE6B. These results suggest that CRX may be partially compensated *in vivo* by another member of the Otx transcription factor family. These results are consistent with results reported in the characterization of the *Crx-/-* mouse strain (57). In that study, Furukawa et al., demonstrated by northern blot that the transcripts of several photoreceptor-specific genes were diminished, such as rhodopsin for which a 92% decrease in expression in *Crx-/-* 10-day-old mouse retina samples was shown as compared with wild-type mice of the same age. This is a more dramatic reduction in rhodopsin than was found in the present study (Table 7), in which a decrease of only 50% was seen in rhodopsin transcription as compared to age-matched controls. One possible explanation is that the rhodopsin transcript level in the control mouse sample used was not as high as expected, given that rhodopsin is the most abundant protein in the outer segment of the retina (Table 7). If this is so, then all ratios based on this sample would be overestimated. Furthermore, it has been shown that multiple rhodopsin transcripts of different lengths are present at different levels in the developing mouse (72). It is possible that primers used in this study preferentially amplify cDNA

corresponding to a more abundant transcript than the transcript detected by the northern blot probes in the Furukawa et al. study.

Likewise, PDE6B showed different results in our study in that the transcript level was increased by approximately 25% over the control. The Furukawa et al. study demonstrated a reduction in PDE6B (25%). Our result for PDE6B, however, is probably due to the fact that our control mouse RNA is actually heterozygous for the mutation in the PDE6B gene, *rd*, that causes selective degradation of PDE6B mRNA (73). Thus, we would expect intermediate levels of PDE6B because only the wild-type allele produces stable mRNA, and this would cause the control levels to be artificially low. In fact, if the GAPDH-normalized value of PDE6B were doubled for the control sample, the ratio to the average *Crx-/-* GAPDH-normalized value would be approximately 20%, close to the result in the Furukawa et al. study (Table 7).

The result that PDE6A is reduced by approximately 40% compared with the normal control is an important result in that CRX is important in efficient transcription of the PDE6A gene in mouse; however, it is not essential. The mobility shift assays clearly showed that cellular proteins can bind to the CBE site within the promoter, so any protein that is binding can potentially regulate the gene, whether positively or negatively. These results further emphasize redundancy in cellular control. Furthermore, these results also suggest that minimal expression of CRX is needed to maintain photoreceptor health, possibly because the genes are already expressed but only near threshold quantities in the absence of CRX. That is, if a low-expressing PDE6A or PDE6B transgene were added to a CRX-deficient strain, it might result in enough expression to drive levels over the

minimum concentration required to function. The PDE6A gene promoter has been shown previously to be a weak promoter (74).

Further experiments will determine whether CRX is the most effective transcription factor for PDE6A expression. Further experiments may also show that expression resulting from the interaction of other Otx family members is not sufficient in maintaining the photoreceptor health; that is, we know that the retina will eventually degenerate and that degeneration may be due to the absence of CRX in later stages beyond development. However, other groups have proposed that it is the paucity of rhodopsin in the photoreceptor outer segments that leads to photoreceptor degeneration. It is known that a lack of functional rhodopsin is highly deleterious to photoreceptors since it is the major protein in photoreceptors, accounting for more than 85% of the total protein. In the absence or extremely reduced amounts of rhodopsin, the outer segments of the photoreceptors cannot develop or function properly. It is also proposed that death of large numbers of photoreceptors can cause subsequent death of the retina, although the mechanism is unknown.

Specific Aim 2

It is clear that CRX and NRL are transactivating the proximal promoter of PDE6A in transient transfection studies. It is also clear that CRX and NRL are somehow working together to produce a synergistic effect on expression of the reporter gene. However, because of the limitations of the method, such as naked DNA versus chromatin, it is not clear how this relates to the actions of these molecules *in vivo*. In co-transfections using the mutated binding sites M13 (TATA) and M16 (CBE), it was shown

by reduced levels of expression that the correct sequence is necessary for normal, efficient expression. Nevertheless, expression occurred when CRX and/or NRL were added to the experiment, suggesting that there is some binding to the site regardless of consensus sequence, or that CRX and/or NRL stimulate endogenous transcription factor genes that upregulate expression. The CBE site mutation M16 was more affected by the sequence change, in that expression was low (30-50%) for M16 but was high (120-140%) for M13 compared to pGL3-300 (Fig. 17). This may suggest that this promoter is still under constitutive control at the TATA-like box (i.e., 30-50% expression because of TATA-directed transcription when CRX cannot bind to the CBE site). This may also suggest that CRX has a small influence on the TATA-like site, which contains the core of the CRX binding sequence, TAAT. In footprinting studies, it was shown that CRX was able to protect a large region of the PDE6A promoter, including the CBE site, the TATA-like site, and a third conserved site similar to the NRE (Fig. 6). Transfection results from the mutated plasmids may then suggest that CRX is able to bind and/or influence more than one site and that expression driven by a mutated construct occurs due to binding of CRX at the other of two sites in the promoter. The differences in expression between M13 and M16 constructs may indicate differences in CRX binding affinity or position effects of CRX binding; that is, CRX prefers the CBE to TATA or NRL sites.

Another explanation for the large increase in expression with the M13 plasmid may be NRL binding alone. It has been shown that NRL is able to bind ubiquitous basic zipper protein transcription factors such as c-fos and c-jun (45). Heterodimers of these proteins can bind to AP1 sites and enhance transactivation of a promoter. The AP1-like site is within the region of the M16 mutation and remains unaltered. Perhaps heterodi-

mers are binding within the region to promote increased transcription from the TATA site. Furthermore, the M16 plasmid is expressed at a higher fold-stimulation when NRL is added than when CRX is added, which is converse for the other plasmids. Expression is increased with CRX and NRL over NRL alone; however, this can be explained by a cooperative binding scheme in which CRX bound to NRL through the homeodomain and zipper domains, possibly leading to the assembly of the transcription complex (46).

An interesting result in this study is that the M13 plasmid, that is, the TATA-like site mutation, shows a very large synergistic effect when both CRX and NRL are added together. We show that CRX is able to bind the TATA-like region (Fig. 21). Perhaps the proximity of this site to the NRE-like site facilitates recruitment of NRL to heterodimerize with CRX in the TATA site and enhances activation of the reporter because of this dimer.

The results of the EMSAs support the data obtained from transient transfection studies. Through band shift analysis, it has been shown that the addition of CRX causes a specific shift in general transcription factor binding to a characteristic band or bands that depends on the size of the oligonucleotide tested. The specificity of these shifts is supported by competition assays in which specific bands were competed away from CRX by unlabeled self-competitor. Furthermore, a hierarchy of binding sites could be determined on the basis of the relative strengths of competition among the different oligonucleotides tested. Moreover, the homeodomain binding experiment revealed variations in binding efficiencies for the oligonucleotides that were used in the experiment (Fig. 24). The CBE site was consistently strongest in competition, in that oligonucleotides containing this site were able to strongly compete away oligonucleotides not containing this site

(TATA, NRE, Fig. 21). The TATA site was also able to bind CRX, but was able to compete only moderately against CBE. The M16/M13 oligonucleotide did not even bind CRX (Fig. 22). The AP1 site demonstrated no benefit to the binding of CRX or to the binding of CRX and NRL together (Fig. 23).

These results support the positive transfection results and demonstrate that CRX has a direct effect on the PDE6A promoter fragments in the reporter plasmids. Expression resulting from CRX transactivation is explained simply by the fact that CRX is binding to the sites within the promoter, and preferentially binding to the CBE site. However, the effect of NRL and the synergistic effect of NRL with CRX are not explained, as no band shift resulted with NRL. It was suspected that NRL was binding the NRL-like site; however, NRL is not binding to this short promoter region, which does not explain the effect of NRL in transient transfection other than as participating in a cooperative binding complex.

A possible role for NRL in PDE6A promoter regulation is as a secondary transcription factor that does not bind DNA. The structure of the basic zipper protein NRL suggests that it has DNA-binding capabilities. The band shift data, however, suggest that it does not bind to oligonucleotide DNA from this short promoter region. It has been shown that NRL and CRX interact physically through the leucine zipper region of NRL and the homeodomain region of CRX (46). This accounts for the highly synergistic effect of rhodopsin activation (46), because two CRX binding sites surround an NRL binding site. Rehemtulla et al. demonstrated specific binding of NRL to the rhodopsin NRE (TGCTGATTCAGCC), which was not apparent when an oligonucleotide with an NRE-like sequence (CTATGATCCTGCC) was used (46). This may be consistent with

our results in that slight sequence changes caused an inability for NRL to bind (PDE6A NRE oligonucleotide, TGATCCTCATAATC).

A second possible role for NRL in the expression of PDE6A is that NRL serves to relieve repression caused by CRX binding. Evidence for this role is circumstantial, however. The effect of CRX or NRL on the promoter fragments is small, between 3- and 7-fold over the reporter plasmid alone (Fig. 15). Also, the internal reporter expression is not entirely reliable, since an effect is seen resulting from the type of plasmid promoter used (data not shown). Therefore, CRX may in fact be inhibiting the expression of the reporter by binding to the sites and blocking transcription by cellular factors. Then when NRL is added, the NRL binds to CRX through the leucine zipper and homeodomain, respectively, and removes the repression caused by CRX. This would account for the synergism seen in cotransactivation studies involving PDE6A and, possibly, PDE6B and rhodopsin. However, the simple fact that a dose response is seen in CRX transactivation (data not shown) can refute this argument, in that if CRX were a repressor, greater repression would be expected as more CRX is added. On the other hand, the standard deviations among experimental trials (errors in figures are given as standard error of the mean) are great enough to include the increase in expression caused by CRX, so this effect may in fact be a relic of transfection method. Furthermore, NRL also shows an effect on expression, and it has been shown that NRL is not even binding to the sequence present in the promoter region. Thus, it may be that this small effect is indeed due not to the transcription factors themselves, but to enhanced overall transcription within the cell. Then, it follows that if CRX is repressing the promoter, then binding of CRX by NRL would help to deter the association of CRX with the binding sites.

The importance of repression by CRX could be developmentally important, in that CRX may postpone expression of specific retinal genes that respond to retina-specific transcription factors that are expressed early in development, such as NRL (72). This may be important to the developing photoreceptor so that enzymes that are not needed will not interfere in the precise structuring of the outer segments. It is thought that mutations in outer segment structural genes such as peripherin and ROM1 cause retinal degenerations because the structure itself cannot support the large amount of rhodopsin expressed in rod cells (75, 76). This implies that early structural development is critical to photoreceptor stability and function. Misexpressed enzymes that are associated with the membrane, such as PDE6, may interfere with organization. However, PDE6 activity coincides with both rhodopsin expression and visible outer segment development in rat, and, furthermore, the PDE6B subunit is expressed earlier than rhodopsin or PDE6A (72). Rhodopsin requires CRX and NRL for expression, and CRX and NRL are expressed before both rhodopsin and PDE6A (77).

Specific Aim 3

There was no expression of the transgene reporter in the retina or any tissue in the mice studied. However, the short promoter is capable of directing transcription, as seen in RT-PCR and *in situ* hybridization results (Figs. 25-26). It has been determined that expression of reporter protein was not seen because of the presence of a secondary upstream initiator codon within the promoter that may have caused the mRNA to have an altered reading frame that resulted in a truncation (data not shown).

The specific PCR products shown in Fig. 25 demonstrate that the transcript is present in the three lines of mice studied because the primers are specific to the engineered plasmid that is not found endogenously. Likewise, the specific probes used in the *in situ* hybridization experiments were generated to be specific to engineered parts of the transgene so that only transcribed transgene would be visible. However, the signal that is detected with the transgene-specific experimental probe in Fig. 26*A* is somewhat reduced when compared with the endogenous PDE6B probe in Fig. 26*C*. This lower signal can be due to several reasons, including that PDE6B is expressed at a higher level than PDE6A endogenously, that the mice studied were heterozygous for the transgene, that the minimal promoter is lacking some element responsible for high expression such as an enhancer, or that the transgene has experienced a degree of repression resulting from integration.

In all transgenic mouse projects, there is the concern that chromatin effects may play a part in expression of transgenes. If the transgene is inserted near heterochromatin, the gene may not be accessed by transcription machinery and, thus, may never be expressed. It is possible that the transgene may be inserted near a repressor region as well. However, it is unlikely, but not impossible, that all three lines of transgenic mice were inhibited because of position effects. It is extremely likely that the altered translation initiation site caused the absence of reporter protein expression.

A transgenic mouse model containing the proximal promoter of PDE6B was recently reported in which expression of the transgene was detected by β-galactosidase reporter assays and immunohistochemical staining. The promoters of the two genes are similar; however, the Ret-1 (CBE) and TATA-like sites are reversed. The authors

reported that expression of PDE6B was seen exclusively in the retina and predominantly in the outer segments of the photoreceptors (69). LacZ expression, however, was detected at levels barely above background staining. Furthermore, tissue culture studies show that the PDE6B promoter *in vitro* is five to ten times stronger than the PDE6A promoter (B. White, personal communication). This may explain the detection differences in PDE6A transgene studies as compared with PDE6B studies: Because the PDE6A promoter is at least five times weaker than the PDE6B promoter, PDE6A-driven transcription and LacZ expression may not be detectable if PDE6B-driven LacZ expression is barely significant above background levels *in vivo*.

CONCLUSIONS

The results of this study suggest that the proximal promoter of the PDE6A gene is responsive to the transcription factors CRX and NRL. A short promoter of 300 base pairs is sufficient to drive photoreceptor-specific expression in cell culture (i.e., using photoreceptor-specific transcription factors) and *in vivo* in transgenic mice. Although CRX appears to be important in expression, as shown by mutation studies, the absence of CRX in the knockout model does not prevent the expression of PDE6A, and, in fact, allows approximately 60% of normal PDE6A expression. Thus, the results suggest that CRX is necessary for high levels of expression of PDE6A, but is not sufficient and not absolutely required for photoreceptor-specific expression in the young mouse. Retinal degeneration in adult *Crx-/-* mice prevents study of CRX deficiency in later stages. Perhaps the rapid degeneration of photoreceptors in the CRX knockout mice suggests the role of CRX is not in development, but in maintenance of the photoreceptor after maturation.

The results of this study show promise in the role of the PDE6A promoter in gene therapy of retinal disease. The weakness of the promoter allows moderate expression of a reporter protein in *in vitro* systems: In photoreceptor cells in which rhodopsin is the most abundant protein and structure is highly important, another overexpressed protein could hinder the proper functioning of the cell. This study also demonstrated that the PDE6A promoter is activated specifically in retinal cells *in vivo* and responds to photoreceptor-specific transcription factors. These characteristics make the PDE6A promoter

ideal for targeted gene therapy in which a specific tissue is diseased and a specific rescue gene is inserted. New delivery systems for retinal gene therapy, such as the adeno-associated virus method, complement these characteristics in that a specific, prolonged, and low-level gene replacement will be essential to rescuing hereditary retinal diseases. Future experiments will include further characterization of the promoter *in vivo* to obtain a more realistic idea of how the PDE6A promoter acts in its native environment.

REFERENCES

1 Oyster, C. W. (1999) *The Human Eye*, Sinauer Associates, Sunderland, MA

2 Dowling, J. E. (1987) *The Retina*, Harvard University Press, Cambridge, MA

3 Molday, R. S. (1998) *Invest. Ophthalmol. Vis. Sci.* **39**, 2493-2513

4 Schwartz, S. H. (1999) *Visual Perception: A Clinical Orientation*, Appleton and Lange, Stamford, CT

5 Spaide, R. F. (1999) *Diseases of the Retina and Vitreous*, W. Saunders, Philadelphia, PA

6 Stryer, L. (1991) *J. Biol. Chem.* **266**, 10711-10714

7 Tao, L., Pandey, S., Simon, M. I., and Fong, H. K. W. (1993) *Exp. Eye Res.* **56**, 497-507

8 Ying, S., Fong, S. L., Fong, W. B., Kao, C. W. C., Converse, R. L., and Kao, W. W. Y. (1998) *Curr. Eye Res.* **17**, 777-782

9 Artemyev, N. O., Surendran, R., Lee, J. C., and Hamm, H. E. (1996) *J. Biol. Chem.* **271**, 25382-25388

10 Berger, A. L., Cerione, R. A., and Erickson, J. W. (1999) *Biochemistry* **38**, 1293-1299

11 Natochin, M., and Artemyev, N. O. (1996) *J. Biol. Chem.* **271**, 19964-19969

12 Baehr, W., Devlin, M. J., and Applebury, M. L. (1979) *J. Biol. Chem.* **254**, 11669-11677

13 Deterre, P., Bigay, J., Forquet, F., Robert, M., and Chabre, M. (1988) *Proc. Natl. Acad. Sci. U. S. A.* **85**, 2424-2428

14 Fung, B. K.-K., Young, J. H., Yamane, H. K., and Griswold-Prenner, I. (1990) *Biochemistry* **29**, 2657-2664

15 Artemyev, N. O., and Granozsky, A. E. (2001) *Invest. Ophthalmol. Vis. Sci.* **42**, S186 [abstract]

16 Charbonneau, H., Beier, N., Walsh, K. A., and Beavo, J. A. (1986) *Proc. Natl. Acad. Sci. U. S. A.* **83**, 9308-9312

17 Lipkin, V. M., Khramstov, N. V., Vasilevskaya, I. A., Atabekova, N. V., Muradov, K. G., Gabanov, V. V., Li, T., Johnston, J. P., Volpp, K. J., and Applebury, M. L. (1990) *J. Biol. Chem.* **265**, 12955-12959

18 Ong, O. C., Ota, I. M., Clarke, S., and Fung, B. K. K. (1989) *Proc. Natl. Acad. Sci. U. S. A.* **86**, 9238-9242

19 Anant, J. S., Ong, O. C., Xie, H., Clarke, S., O'Brien, P. J., and Fung, B. K. K. (1992) *J. Biol. Chem.* **267**, 687-690

20 Charbonneau, H., Prusti, R. K., LeTrong, H., Sonnenburg, W. K., Mullaney, P. J., Walsh, K. A., and Beavo, J. A. (1990) *Proc. Natl. Acad. Sci. U. S. A.* **87**, 288-292

21 Mou, H., Grazio, H. J., Cook, T. A., Beavo, J. A., and Cote, R. H. (1999) *J. Biol. Chem.* **274**, 18813-18820

22 Koch, K. W., and Stryer, L. (1988) *Nature* **334**, 64-66

23 Palczewski, K., Subbaraya, I., Gorczyca, W. A., Hebekar, B. S., Ruiz, C. C., Ohguro, H., Huang, J., Zhao, X., Crabb, J. W., and Johnson, R. S. (1994) *Neuron* **13**, 395-404

24 Dizhoor, A. M., Olshevskaya, E. V., Henzel, W. J., Wong, S. C., Stults, J. T., Ankoudinova, I., Hurley, J. B. (1995) *J. Biol. Chem.* **270**, 25200-25206

25 Lodish, H., Baltimore, D., Berk, A., Zipursky, S. L., Matsudaira, P., Darnell, J. (1995) *Molecular Cell Biology*, (3rd ed.) W. H. Freeman & Co., New York, NY

26 Carey, M. and Smale, S. T. (2000) *Transcriptional Regulation in Eukaryotes: Concepts, Strategies, and Techniques*, Cold Spring Harbor Laboratory Press, New York, NY

27 Quinn, J. P. (1996) *Prog. Neurobiol.* **50**, 363-379

28 Morrow, E. M., Furukawa, T., and Cepko, C. L. (1998) *Trends Cell Biol.* **8**, 353-358

29 Livesey, F. J., Furukawa, T., Steffen, M. A., Church, G. M., and Cepko, C. L. (2000) *Curr. Biol.* **10**, 301-310

30 Mohamed, M. K., Taylor, R. E., Feinstein, D. S., Huang, X., and Pittler, S. J. (1998) *J. Molec. Neurosci.* **10**, 235-250

31 DiPolo, A., Rickman, C. B., and Farber, D. B. (1996) *Invest. Ophthalmol. Vis. Sci.* **37**, 551-560

32 Wang, Y., Macke, J. P., Merbs, S. L., Zack, D. J., Klaunberg, B., Bennett, J., Gearhart, J., and Nathans, J. (1992) *Neuron* **9**, 429-440

33 Ueda, Y., Iwakabe, H., Masu, M., Suzuki, M., and Nakanashi, S. (1997) *J. Neurosci.* **17**, 3014-3023

34 Morris, T. A., and Fong, S. L. (1993) *Genomics* **17**, 442-448

35 Chen, S., and Zack, D. J. (1996) *J. Biol. Chem.* **271**, 28549-28551

36 Chen, S., Wang, Q. L., Nie, Z., Sun, H., Lennon, G., Copeland, N. G., Gilbert, D. J., Jenkins, N. A., and Zack, D. J. (1997) *Neuron* **19**, 1017-1030

37 Morabito, M. A., Yu, X., and Barnstable, C. J. (1991) *J. Biol. Chem.* **266**, 9667-9672

38 Kimura, A., Singh, D., Wawrousek, E. F., Kikuchi, M., Nakamura, M., and Shinohara, T. (2000) *J. Biol. Chem.* **275**, 1152-1160

39 Fong, S. L., and Fong, W. B. (1999) *Curr. Eye Res.* **18**, 283-291

40 Catron, K. M., Iler, N., and Abate, C. *Molec. Cell Biol.* **13**, 2354-2365

41 Boatright, J. H., Borst, D. E., Peoples, J. W., Bruns, J., Edwards, C. L., Si, J. S., and Nickerson, J. M. (1997) *Mol. Vis.* **3**, 15

42 Ahmad, I., Yu, X., and Barnstable, C. J. (1994) *J Neurochem.* **62**, 396-399

43 Martinez, J. A., and Barnstable, C. J. (1998) *Biochem. Biophys. Res. Comm.* **250**, 175-180

44 Bovolenta, P., Mallemaci, A., Briata, P., Corte, G., Boncinelli, E. (1997) *J. Neurosci.* **17**, 4243-4252

45 Kerppola, T. K., and Curran, T. (1994) *Oncogene* **9**, 675-684

46 Rehemtulla, A., Warwar, R., Kumar, R., Ji, X., Zack, D. J., and Swaroop, A. (1996) *Proc. Natl. Acad. Sci. U. S. A.* **93**, 191-195

47 Li, X., Chen, S., Wang, Q., Zack, D. J., Snyder, S. H., and Borjigen, J. (1998) *Proc. Natl. Acad. Sci. U. S. A.* **95**, 1876-1881

48 Kumar, R., Chen, S., Scheurer, D., Wang, Q. L., Duh, E., Sung, C. H., Rehemtulla, A., Swaroop, A., Adler, R., and Zack, D. J. (1996) *J. Biol. Chem.* **271**, 29612-29618

49 Kikuchi, T., Raju, K., Breitman, M. L., and Shinohara, T. (1993) *Mol. Cell Biol.* **13**, 4400-4408

50 Yu, X., Leconte, L., Martinez, J. A., and Barnstable, C. J. (1996) *J. Neurochem.* **67**, 2494-2504

51 Shaaban, S. A., and Deeb, S. S. (1998) *Invest. Ophthalmol. Vis. Sci.* **39**, 885-896

52 Lin, Z. Y., Li, G. R., Takizawa, N., Si, J. S., Gross, E. A., Richardson, K., Nickerson, J. M. (1997) *Mol. Vis.* **3**, 17

53 Breitman, M. L., Tsuda, M., Usukura, J., Kikuchi, T., Zucconi, A., Khoo, W., Shinohara, T. (1991) *J. Biol. Chem.* **266**, 15505-15510

54 Bobola, N., Hirsch, E., Albini, A., Altruda, F., Noonan, D., Ravazzolo, R. (1995) *J. Biol. Chem.* **270**, 1289-1294

55 Cepko, C. L., Austin, C., Yang, X., Alexiades, M., and Ezzedine, D. (1996) *Proc. Natl. Acad. Sci. U. S. A.* **93**, 589-595

56 Vandendries, E. R., Johnson, D., Reinke, R. (1996) *Dev. Biol.* **173**, 243-255

57 Furukawa, T., Morrow, E. M., Li, T., Davis, F. C., and Cepko, C. L. (1999) *Nat. Genet.* **23**, 466-470

58 Freund, C. L., Wang, Q. L., Chen, S., Muskat, B. L., Wiles, C. D., Sheffield, V. C., Jacobson, S. G., McInnes, R. R., Zack, D. J., and Stone, E. M. (1998) *Nat. Genet.* **18**, 311-312

59 Swain, P. K., Chen, S., Wang, Q. L., Affatigato, L. M., Coats, C. L., Brady, K. D., Fishman, G. A., Jacobson, S. G., Swaroop, A., Stone, E., Sieving, P. A., and Zack, D. J. (1997) *Neuron* **19**, 1329

60 Kim, J. S., and Pabo, C. O. (1997) *J. Biol. Chem.* **272**, 29795-29800

61 Mitton, K. P., Swain, P. K., Chen, S., Xu, S., Zack, D. J., and Swaroop, A. J. (2000) *J. Biol. Chem.* **275**, 29794-29799

62 Lem, J., Applebury, M. L., Falk, J. D., Flannery, J. G., and Simon, M. I. (1991) *Neuron* **6**, 201-210

63 Nie, Z., Chen, S., Kumar, R., and Zack, D. J. (1996) *J. Biol. Chem.* **271**, 2667-2675

64 Zack, D. J., Bennett, J., Wang, Y., Davenport, C., Klaunberg, B., Gearhart, J., and Nathans, J. (1991) *Neuron* **6**, 187-199

65 Yu, X., Chung, M., Morabito, M. A., and Barnstable, C. J. (1993) *Biophys. Res. Commun.* **191** 76-82

66 Boatright, J. H., Buono, R., Bruno, J., Lang, R. K., Si, J. S., Shinohara, T., Peoples, J. W., and Nickerson, J. M. (1997) *Exp. Eye Res.* **64**, 269-277

67 Mani, S. S., Besharse, J. C., and Knox, B. E. (1999) *J. Biol. Chem.* **274**, 15590-15597

68 DiPolo, A., Lerner, L. E., and Farber, D. B. (1997) *Nucl. Acids Res.* **25**, 3863-3867

69 Ogueta, S. B., DiPolo, A., Flannery, J. G., Yamashita, C. K., and Farber, D. B. (2000) *Invest. Ophthalmol. Vis. Sci.* **41**, 4059-4063

70 Baehr, W., Champagne, M. S., Lee, A. K., and Pittler, S. J. (1991) *FEBS Lett.* **278**, 107-114

71 Taylor, R. E., Shows, K. H., Zhao, Y., Pittler, S. J. (2001) *Biochem. Biophys. Res. Comm.* **282**, 543-547

72 He, L., Campbell, M. L., Srivastava, D., Blocker, Y. S., Harris, J. R., Swaroop, A., Fox, D. A. (1998) *Mol. Vis.* **4**, 32

73 Yan, W., Lewin, A., and Hauswirth, W. (1998) *Invest. Ophthalmol. Vis. Sci.* **39**, 2529-2536

74 White, J. B., Taylor, R. E., and Pittler, S. J. (2001) *J. Neurosci. Methods* **106**, 1-7

75 Humphries, P., Kenna, P., and Farrar, G. J. (1992) *Science* **256**, 804-807

76 Kajiwara, K., Berson, E. L., and Dryja, T., P. (1994) *Science* **264**, 1604-1608

77 Bibb, L. C., Holt, J. K. L., Tarttelin, E. E., Hodges, M. D., Gregory-Evans, K., Rutherford, A., Lucas, R. J., Sowden, J. C., Gregory-Evans, C. Y. (2001) *Human Mol. Genet.* **10**, 1571-1579

APPENDIX

IACUC APPROVAL

UAB THE UNIVERSITY OF ALABAMA AT BIRMINGHAM

Office of the Provost

NOTICE OF APPROVAL

DATE: May 2, 2001

TO: Steven J. Pittler, Ph.D.
WORB 644 4390
FAX: 934-5725

FROM: Clinton J. Grubbs, Ph.D., Chairman
Institutional Animal Care and Use Committee

SUBJECT: Structure and Regulation of Retinal cGMP PDE Alpha Gene (NIH) 010404662

On April 25, 2001, the University of Alabama at Birmingham Institutional Animal Care and Use Committee (IACUC) reviewed the animal use proposed in the above referenced application. It approved the use of the following species and numbers of animals:

Species	Use Category	Number in Category
Mice	B	2000

Animal use is scheduled for review one year from April 25, 2001. Approval from the IACUC must be obtained before implementing any changes or modifications in the approved animal use.

Please keep this record for your files, and forward the attached letter to the appropriate granting agency.

Refer to Animal Protocol Number (APN) 010404662 when ordering animals or in any correspondence with the IACUC or Animal Resources Program (ARP) offices regarding this study. If you have concerns or questions regarding this notice, please call the IACUC office at 934-7692.

Institutional Animal Care and Use Committee
B10 Volker Hall
1717 7th Avenue South
205.934.7692 • Fax 205.934.1188
iacuc@uab.edu
www.uab.edu/iacuc

The University of
Alabama at Birmingham
Mailing Address:
VH B10
1530 3RD AVE S
BIRMINGHAM AL 35294-0019

GRADUATE SCHOOL
UNIVERSITY OF ALABAMA AT BIRMINGHAM
DISSERTATION APPROVAL FORM
DOCTOR OF PHILOSOPHY

Name of Candidate Kathryn Hanson Shows

Graduate Program Vision Science

Title of Dissertation Characterization of the Human Rod Photoreceptor Cyclic GMP Phosphodiesterase Alpha Subunit Gene Promoter

I certify that I have read this document and examined the student regarding its content. In my opinion, this dissertation conforms to acceptable standards of scholarly presentation and is adequate in scope and quality, and the attainments of this student are such that she may be recommended for the degree of Doctor of Philosophy.

Dissertation Committee:

Name		Signature
Thomas Norton	**, Chair**	
Steven J. Pittler		
Om Srivastava		
Trygve Tollefsbol		
Shu-Zhen Wang		

Director of Graduate Program

Dean, UAB Graduate School

Date 1/24/02